Исследование особенностей взаимодействия компонент климатической системы Арктики по результатам численного моделирования

Платов Г. А., Голубева Е. Н. , Крупчатников В. Н.,
Боровко И.В., Крайнева М.В., Якшина Д.Ф.

Институт вычислительной математики и математической геофизики,
СО РАН, Новосибирск

Роль Арктики в системе Мирового океана

Schematic diagram of the global ocean circulation pathways, the ’conveyer’ belt

(after W.Broecker, modified by E.Maier-Reimer)

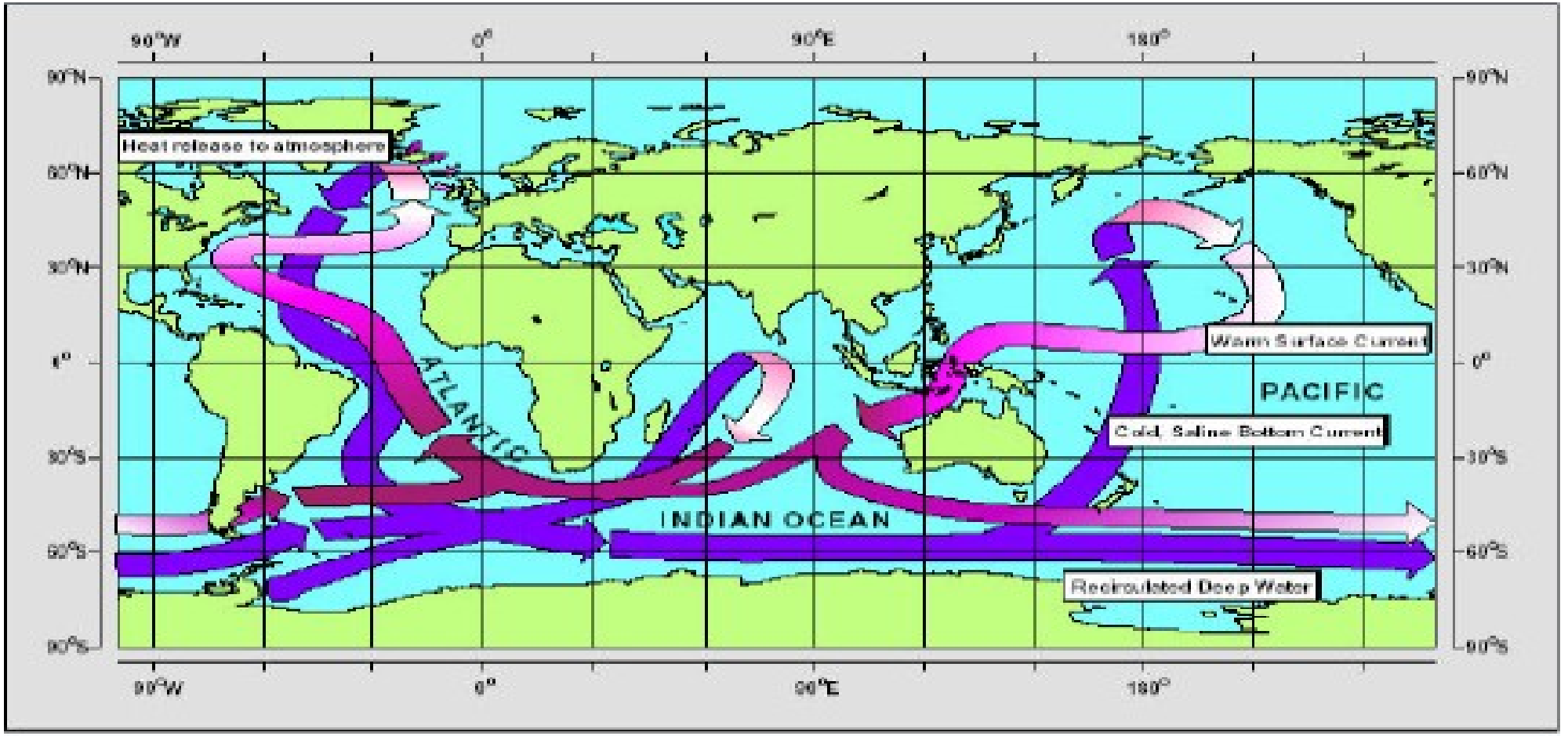

Schematic diagram of the global ocean circulation pathways, the 'conveyer' belt (after W. Broecker, modified by E. Maier-Reimer).

Глобальное потепление

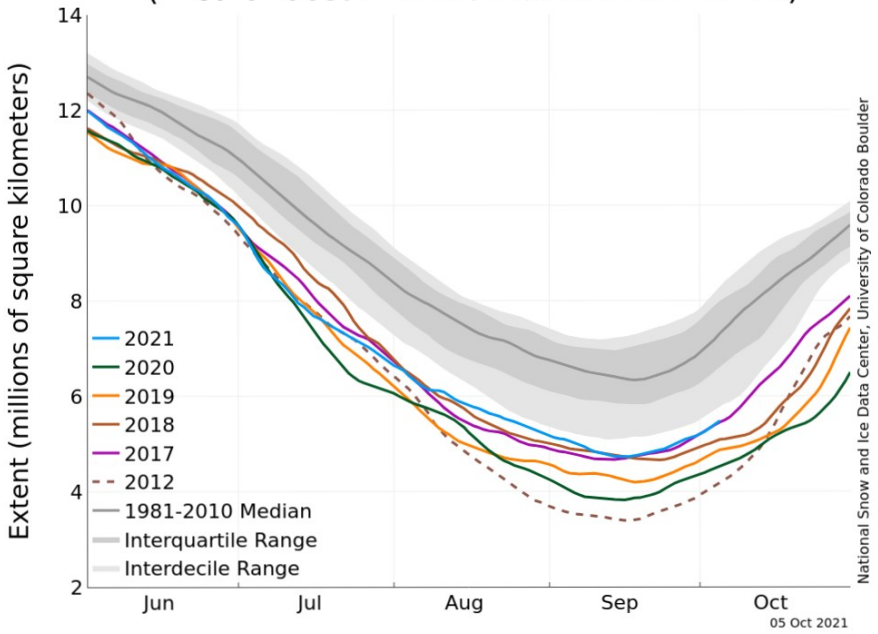

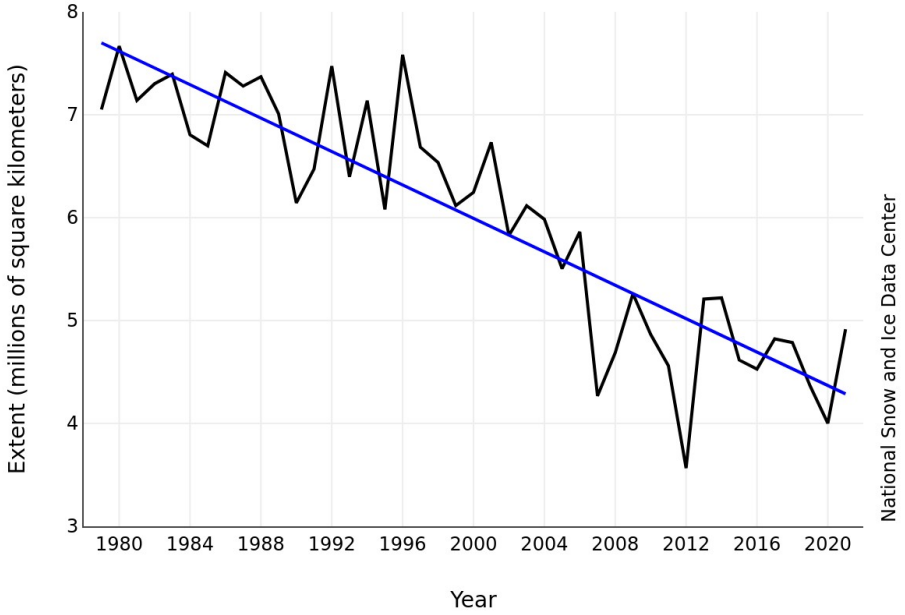

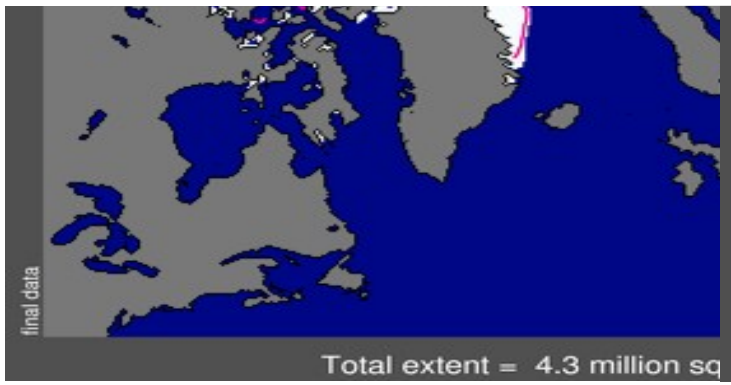

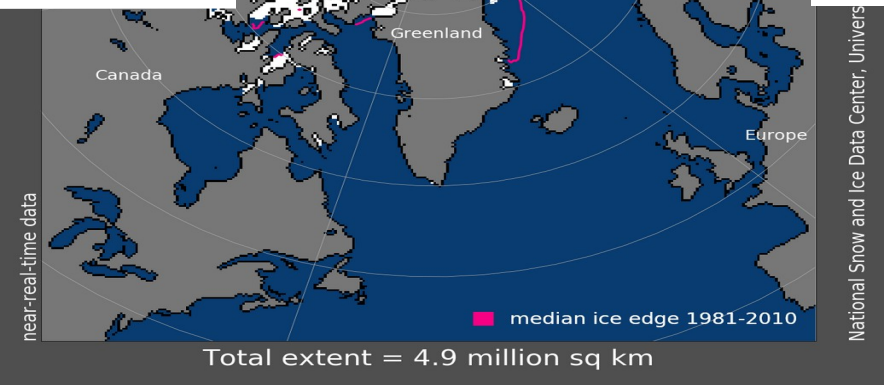

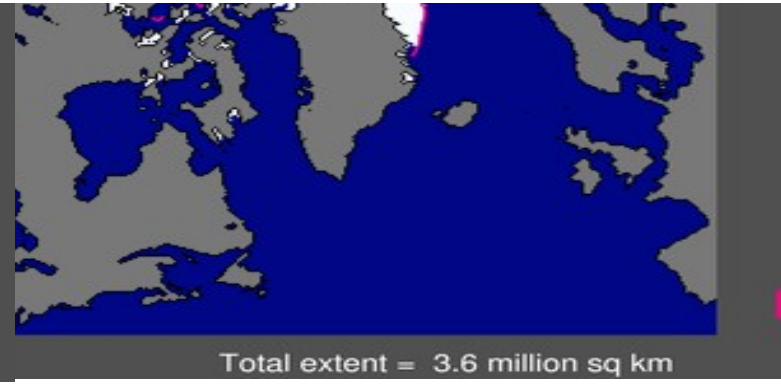

Проекты

- Проект НИР 0215-2021-0003 "Математические модели физики атмосферы, гидросферы, экологии и методы решения прямых и обратных задач с усвоением данных, задач дистанционного зондирования Земли для исследования климата, природных и техногенных воздействий на окружающую среду." Руководители: д.ф.-м.н. Платов Г.А., д.ф.-м.н. Пененко В.В.
- Проект РНФ № 19-17-00154 "Исследование взаимодействия компонент системы атмосфера-океан-морской лед арктического региона в условиях изменений глобального климата«. Руководитель– д.ф.-м.н. Платов Г. А. (отв. исп.: д.ф.-м.н. Крупчатников В. Н., д.ф.-м.н. Голубева Е. Н.)
- Проект РНФ № 20-11-20112 «Разработка системы моделирования для анализа современного состояния и оценки тенденций будущих изменений природной среды Сибирских шельфовых морей» Руководитель д.ф.-м.н. Голубева Е. Н (отв. исп.: д.ф.-м.н. Чеверда В. А., д.ф.-м.н. Решетова Г. В., к.ф.-м.н. Малахова В. В.)
- Проект РФФИ № 20-05-00536 «Исследование роли арктических шельфовых морей в формировании ледовых и гидрологических полей Северного Ледовитого океана в условиях меняющегося климата Земли» Руководитель – д.ф.-м.н. Голубева Е.Н.
- Проект РФФИ №20-05-00241 «Модельная оценка выделения метана из донных отложений Арктики в атмосферу в прошлом и будущем» Руководитель – к.ф.-м.н. Малахова В. В.
- Проект CRiceS “Climate relevant interactions and feedbacks: the key role of sea ice and snow in the polar and global climate system” (H2020-LC-CLA-2020-2/Building a low-carbon, climate resilient future: climate action in support of the Paris Agreement). Руководитель группы: д.ф.-м.н. Платов Г. А.

Схема комплекса моделей

- Замена блоков
- Использование моделей данных
- Режим записи/воспроизведения блока взаимодействия

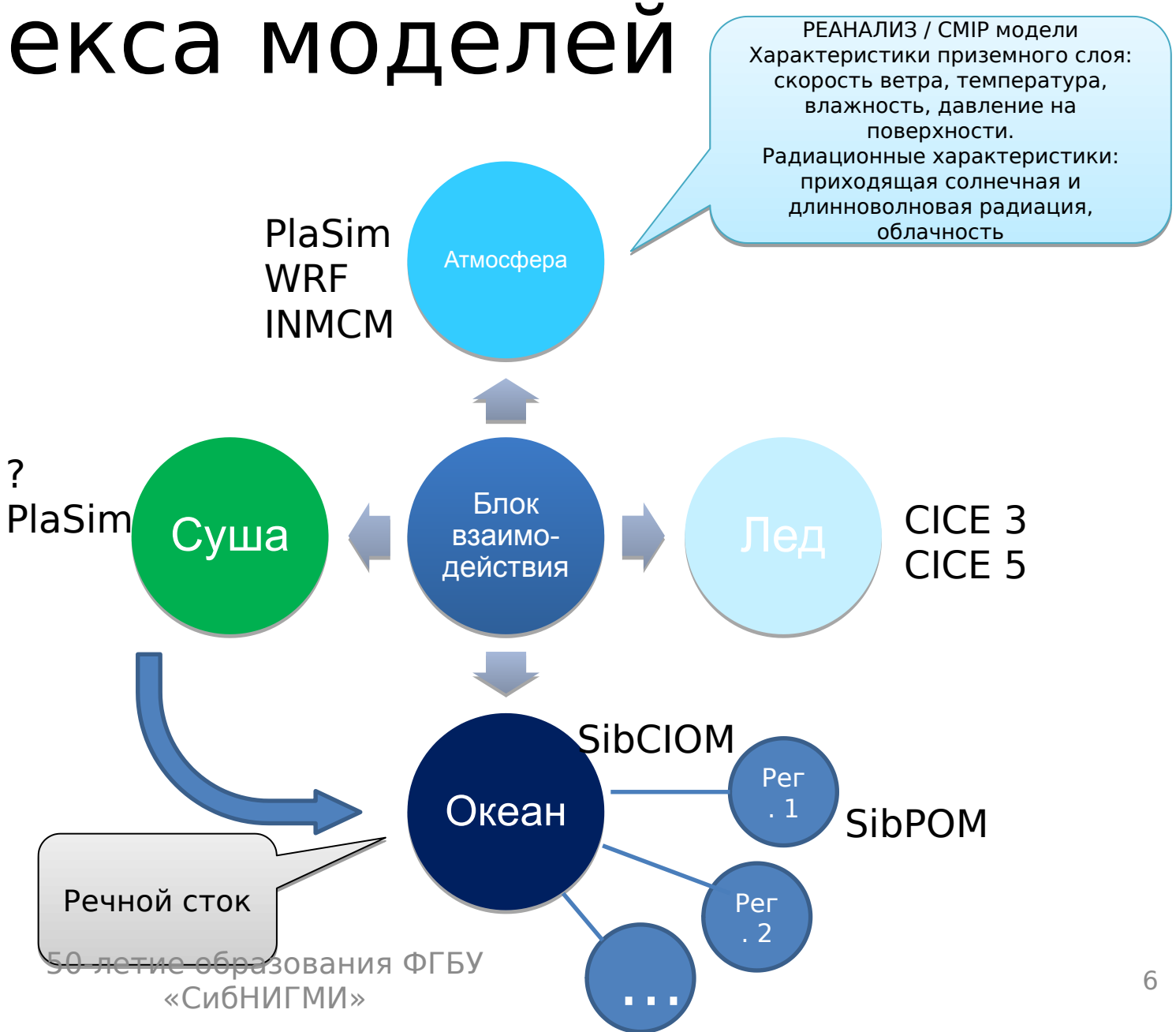

Система совместных и вложенных моделей SibCIOM

- Модель общей циркуляции океана ИВМиМГ СОРАН *(Кузин 1982, Голубева и др. 1992, Golubeva and Platov, 2002)*
- Ice model-CICE 3.1 (elastic-viscous-plastic)
  (W.D.Hibler ,1979, E.C.Hunke, J.K.Dukowicz,1997, G.A.Maykut 1971 C.M.Bitz, W.H.Lipscomb 1999,J.K.Dukowicz, J.R.Baumgardner 2000, W.H.Lipscomb, E.C.Hunke 2004)

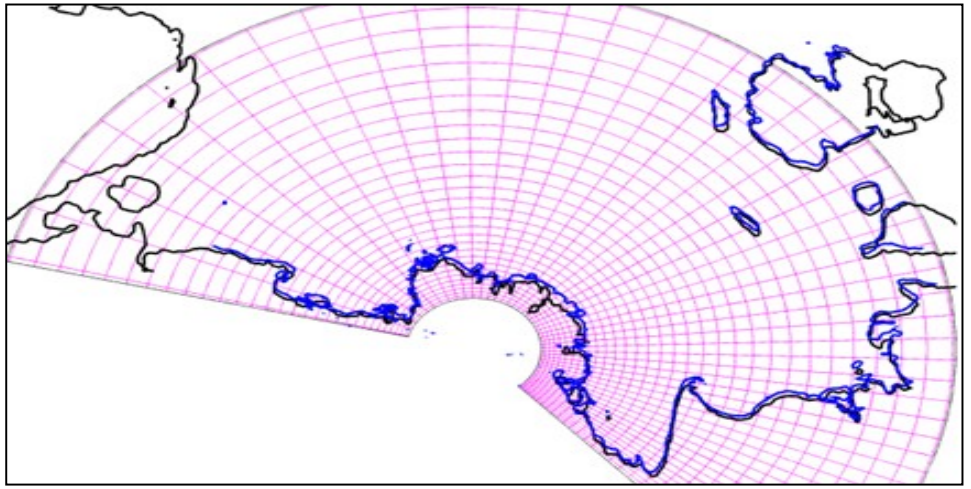

- POM (Princeton ocean model), вложенная в модель ИВМиМГ -- SibPOM
  - Моделируемый период – до одного года

Блок усвоения данных

- Вертикальные профили температуры и солености – Международный полярный год (IPY-2008)
- Температура поверхности (skin temperature) – спутники AVHRR Pathfinder

Grid and Domain

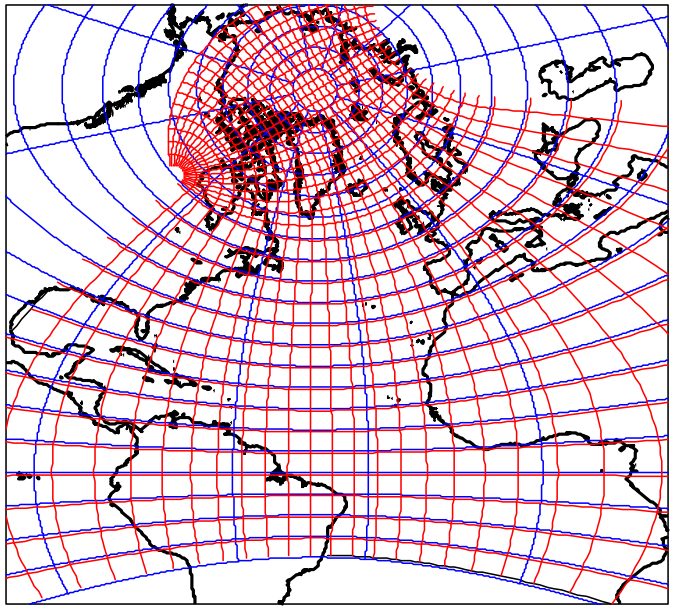

Numerical domain: from 20S Atlantic to Bering Strait

Grid specification: spherical in Atlantic (1°: 1°) + reprojected bipolar grid from 65°N (Ross Murray,1996), 33 vertical levels

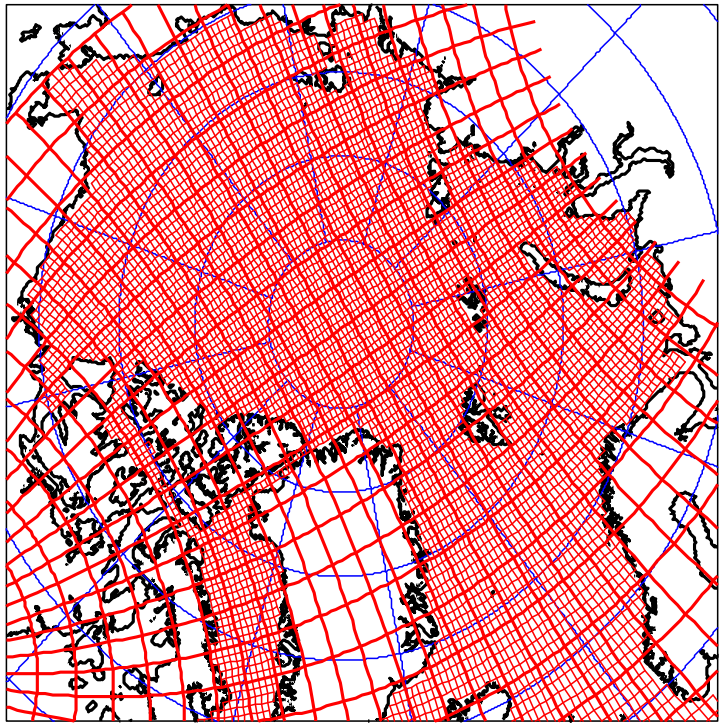

The model domain was built with horizontal resolution of $1x1^0$ in Atlantic. The reprojected bipolar grid in Arctic has minimum spacing equal to 35km while maximum spacing is about 62km.

Уравнения модели льда

$$\frac{\partial g}{\partial t} = -\nabla \cdot (g\mathbf{u}) - \frac{\partial}{\partial h}(fg) + \psi,$$

$g(\boldsymbol{x},h,t)$ – функция распределения льда, $\boldsymbol{x}$ – горизонтальные координаты (x,y), $\nabla = (\frac{\partial}{\partial x}, \frac{\partial}{\partial y})$ итальный градиент, $\mathbf{u}$ – скорость льда, h – толщина льда, f – скорость термодинамического роста, ψ – функция перераспределения в случае торошения.

$$\begin{aligned} \frac{\partial}{\partial t}(a_{in}) + \nabla \cdot (a_{in}\mathbf{u}) &= 0, \\ \frac{\partial v_{in}}{\partial t} + \nabla \cdot (v_{in}\mathbf{u}) &= 0, \\ \frac{\partial v_{sn}}{\partial t} + \nabla \cdot (v_{sn}\mathbf{u}) &= 0. \end{aligned}$$

a_{in} – площадная доля льда, v_{in} – объём льда, v_{sn} – объём снега.

$$\begin{aligned} \frac{\partial (a_{in}T_n)}{\partial t} + \nabla \cdot (a_{in}T_n\mathbf{u}) &= 0, \\ \frac{\partial (v_{in}S_n)}{\partial t} + \nabla \cdot (v_{in}S_n\mathbf{u}) &= 0, \end{aligned}$$

T_n – температура поверхности льда, S_n – энтальпия льда или снега, солёность льда.

Адвекция

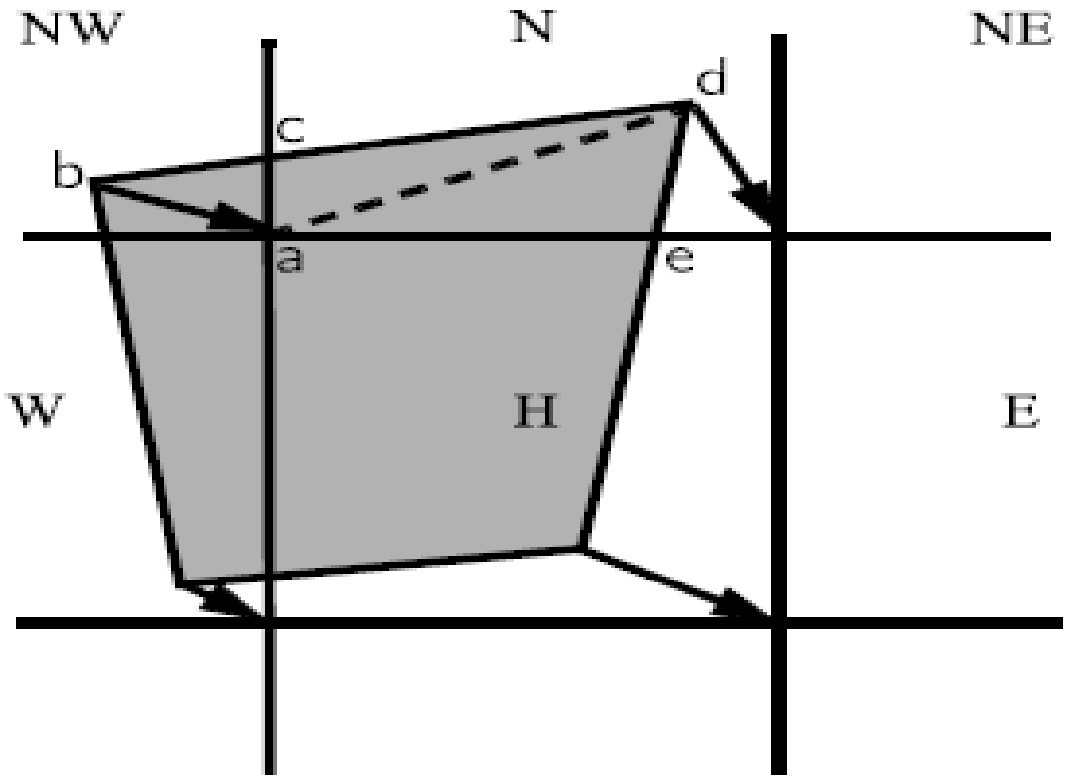

C.M.Bitz, W.H.Lipscomb 1999,J.K.Dukowicz, J.R.Baumgardner 2000, W.H.Lipscomb, E.C.Hunke 2004)

Параллелизация модели льда

CICE-3

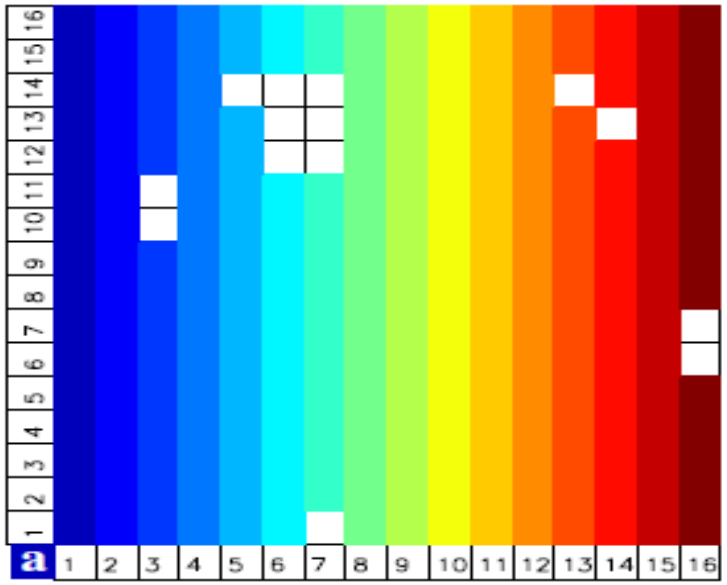

$n_x \times n_y = 310 \times 480$

$(N-1)n_y = 7200$

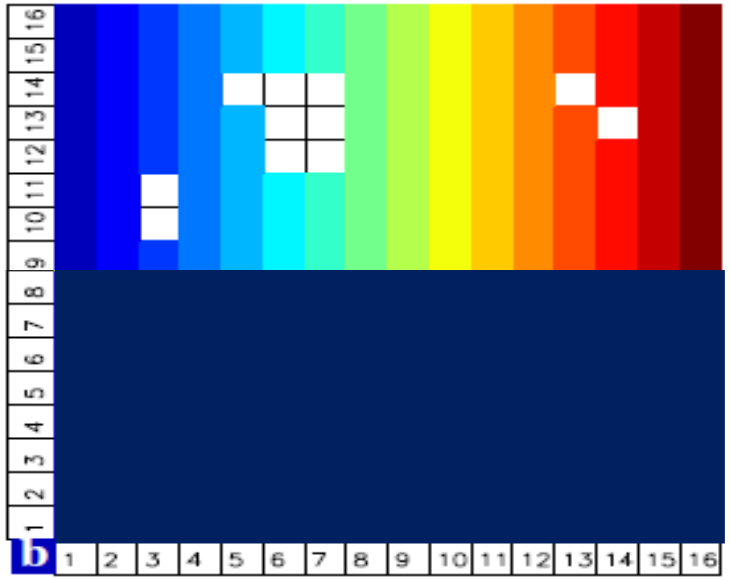

$(N/N_x-1)n_x+(N/N_y-1)n_y=3670$

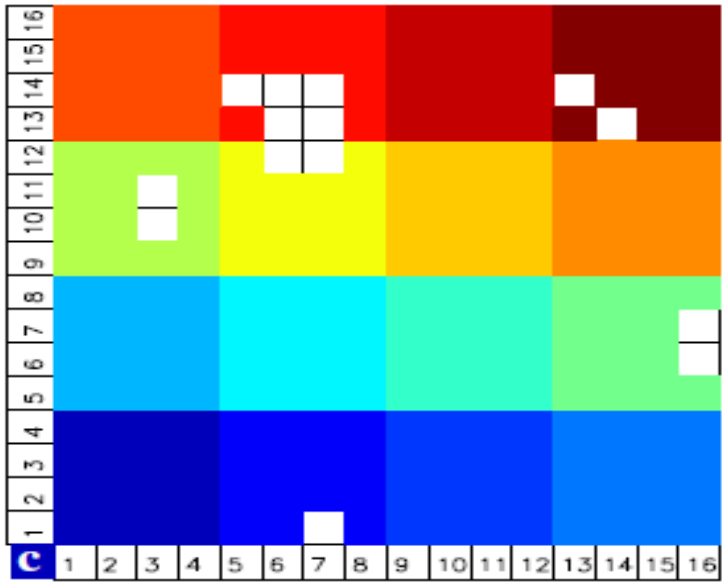

$(N/N_x-1)n_x+(N/N_y-1)n_y=2370$

$n_x+(N-2)n_y/2=3670$

CICE - 5

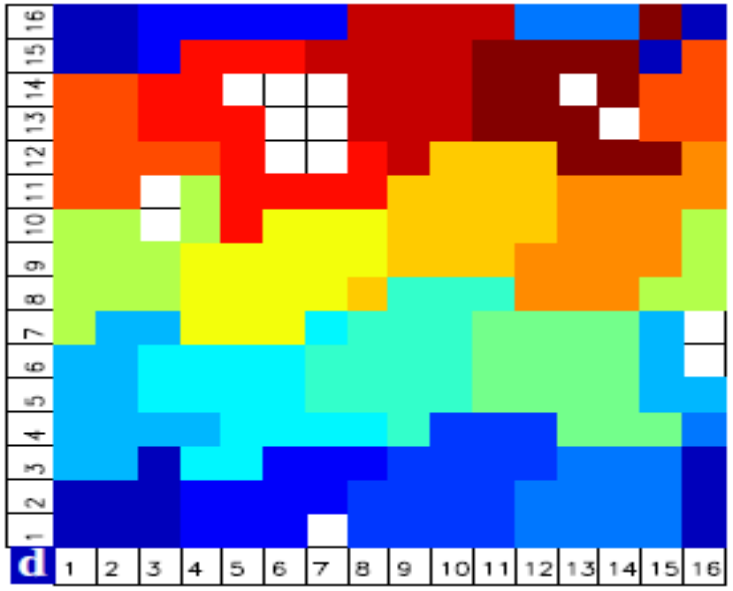

rake with block weighting

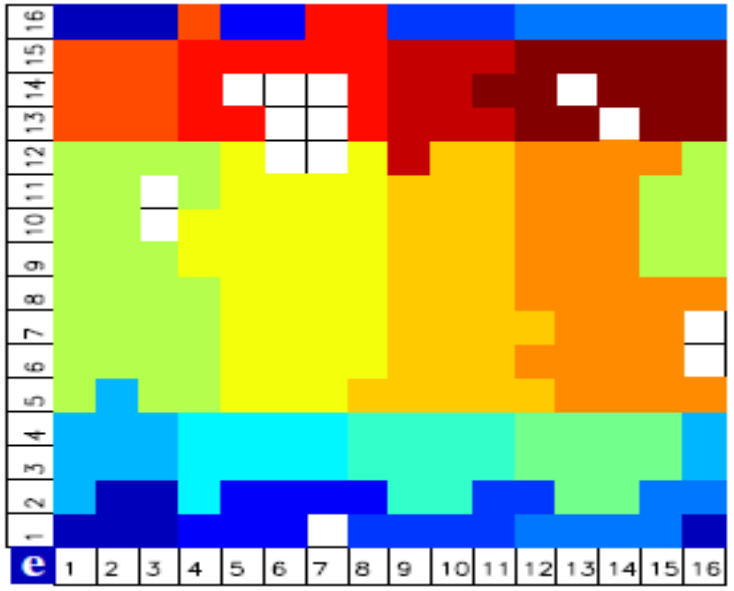

rake with latitude weighting

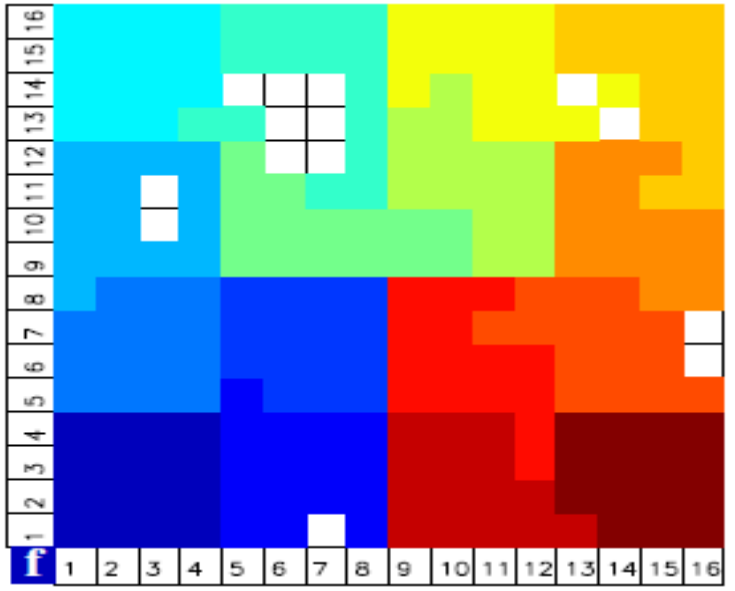

spacecurve

Расчетные характеристики

- Скорость течения – :
  - -- баротропная составляющая для которой вводится функция тока :
  - -- бароклинная составляющая
- Температура и соленость – – активные трассеры
- Пассивные трассеры –
- Лагранжевы частицы

В океанической области Ω в системе криволинейных ортогональных координат ξ_1, ξ_2, z

рассматриваются полные нелинейные уравнения гидротермодинамики океана с учетом приближения гидростатики и Буссинеска для переменных, обозначающих компоненты скорости течения, потенциальную температуру и соленость

$$\frac{\partial u}{\partial t} + L(u) - kv - lv = -\frac{1}{\rho_0 h_1}\frac{\partial p}{\partial \xi_1} + \frac{\partial}{\partial z}\nu_v \frac{\partial u}{\partial z} + F(u, \mu_v),$$

$$\frac{\partial v}{\partial t} + L(v) - ku + lu = -\frac{1}{\rho_0 h_2}\frac{\partial p}{\partial \xi_2} + \frac{\partial}{\partial z}\nu_v \frac{\partial v}{\partial z} + F(v, \mu_v),$$

$$\frac{\partial p}{\partial z} = -\rho g. \qquad \rho = \rho(T, S, p).$$

$$\frac{1}{h_1 h_2}\left[\frac{\partial}{\partial \xi_1}(h_2 u) + \frac{\partial}{\partial \xi_2}(h_1 v)\right] + \frac{\partial w}{\partial z} = 0.$$

$$\frac{\partial T}{\partial t} + L(T) = \frac{\partial}{\partial z}\nu_T \frac{\partial T}{\partial z} + F(T, \mu_T),$$

$$\frac{\partial S}{\partial t} + L(S) = \frac{\partial}{\partial z}\nu_S \frac{\partial T}{\partial z} + F(S, \mu_S),$$

$$L(\phi) = \frac{1}{h_1 h_2}\left[\frac{\partial}{\partial \xi_1}(h_2 u\phi) + \frac{\partial}{\partial \xi_2}(h_1 v\phi)\right] + \frac{\partial}{\partial z}(w\phi),$$

$$F(\phi, \mu) = \frac{1}{h_1 h_2}\left[\frac{\partial}{\partial \xi_1}\left(\mu \frac{h_2}{h_1}\frac{\partial \phi}{\partial \xi_1}\right) + \frac{\partial}{\partial \xi_2}\left(\mu \frac{h_1}{h_2}\frac{\partial \phi}{\partial \xi_2}\right)\right],$$

$$k = \frac{u}{h_1 h_2}\frac{\partial h_1}{\partial \xi_2} - \frac{v}{h_1 h_2}\frac{\partial h_2}{\partial \xi_1}.$$

Модель океана – проблемы параллелизации

- Баротропная составляющая скорости
  - Отказ от неявной схемы
  - Явная – малый шаг по времени
  - Итерации
- Бароклинная составляющая скорости
  - Отказ от неявной схемы
  - Адвекция требует окаймление > 1
- Активные трассеры
- Пассивные трассеры
- Вертикальные процессы
  - Многоточечный носитель из-за параметризаций

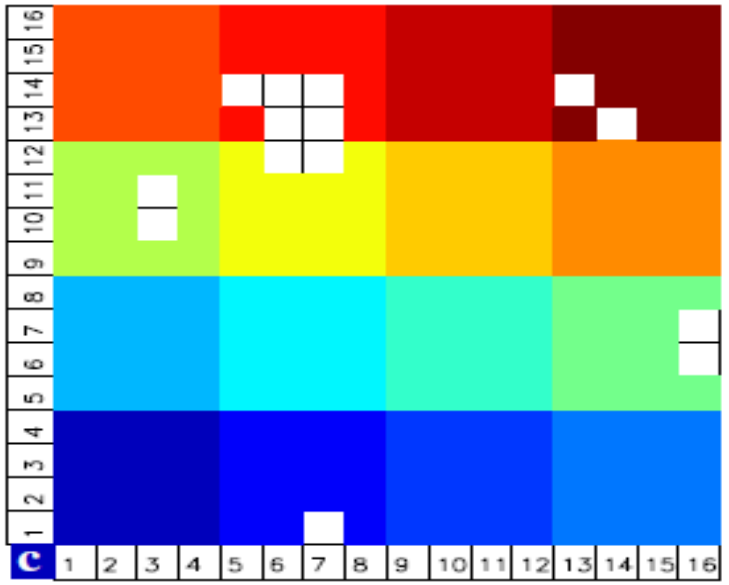

Модель океана – проблемы параллелизации

- Параметризации подсеточных масштабов
  - Вертикальное перемешивание
    - эджастмент
    - глубинная конвекция
    - выделение подледной части
  - Каскадинг
  - Речной сток и жидкие границы
- Ввод – вывод

Частицы-трассеры

- Переход из подобласти в подобласть

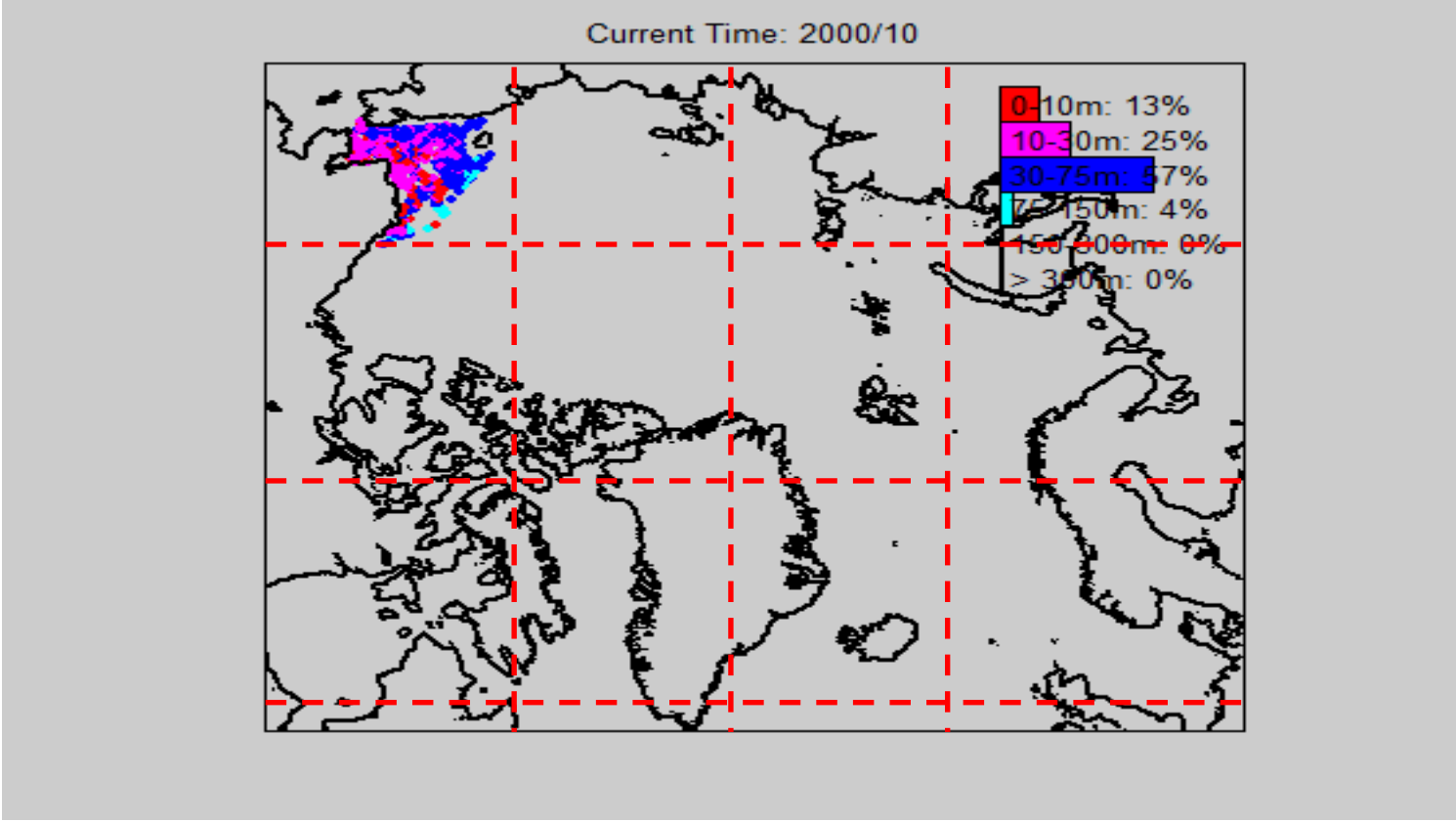

SibCIOM - development

- Increasing model resolution upto ¼ deg
- Global domain + Extending to global climate model (atm, ocn,ice,land)
- Make model resolution optional

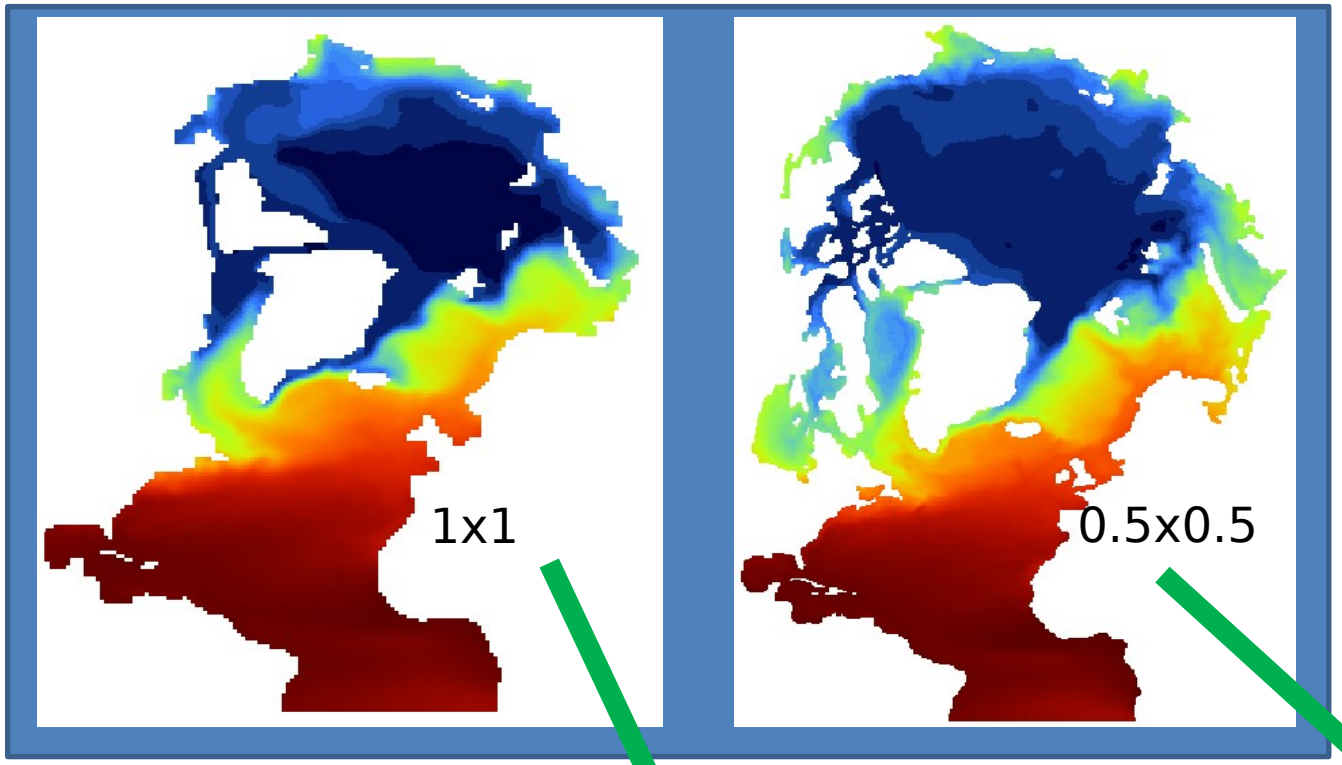

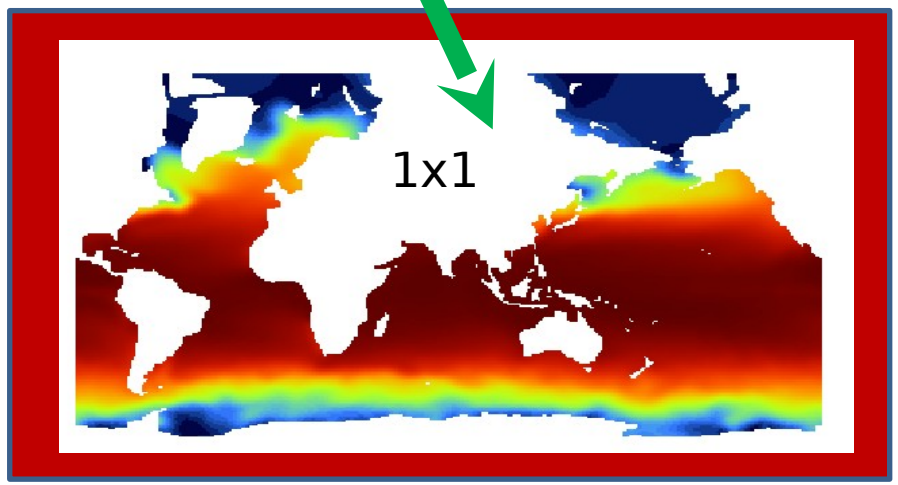

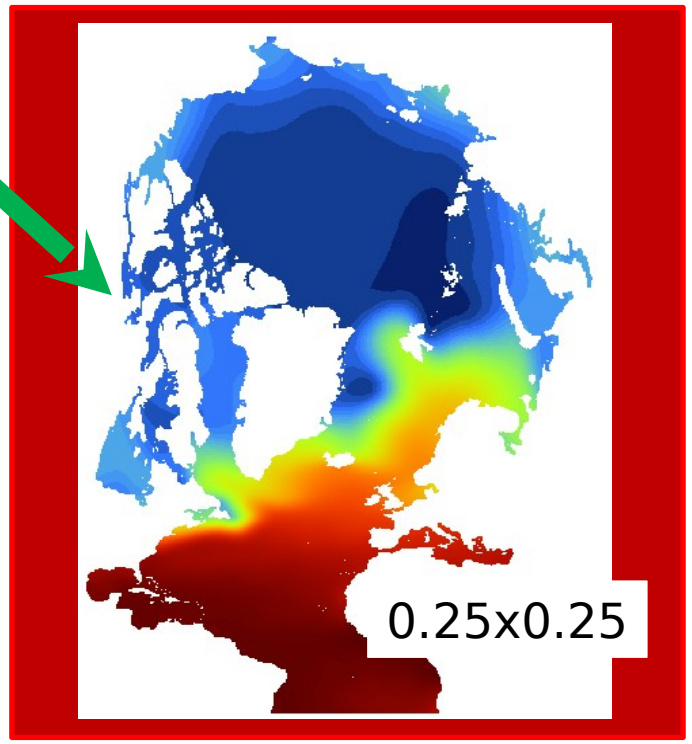

Nested regional model

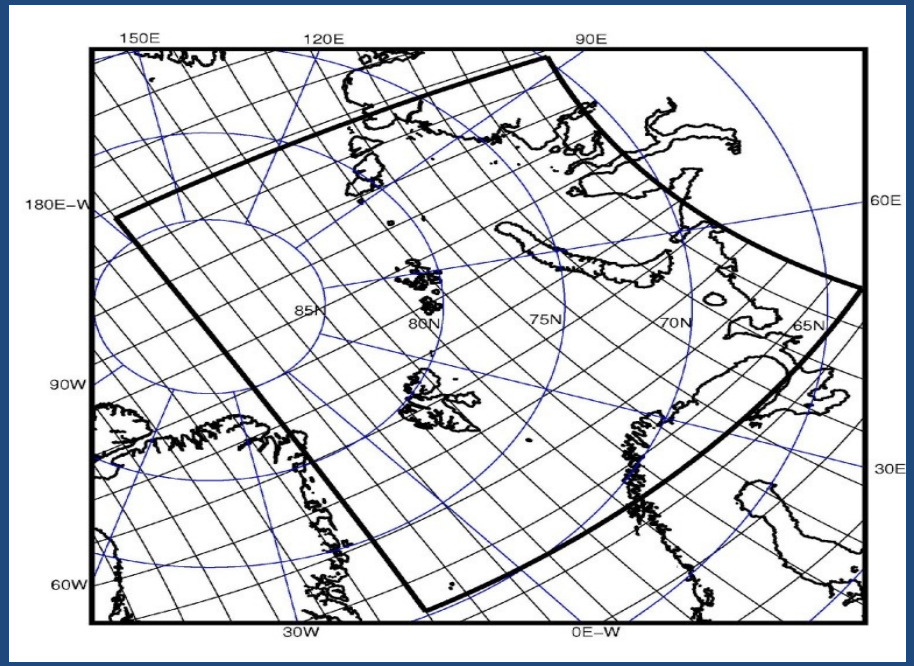

- SibPOM
- Barents and Kara Seas
- Horizontal resolution 2-20 km
- Simulated period – 215 days (Jan-Jul, 1983)

GCM receives from regional model:

- Temperature, salinity (T, S) and barotropic velocity (U, V), via second order relaxation terms

$$\left.\left(\frac{\partial T_0}{\partial t}\right)\right|_{nudging} = \left\{\frac{\partial}{\partial x}\left(A\frac{\partial}{\partial x}\right)+\frac{\partial}{\partial y}\left(A\frac{\partial}{\partial y}\right)\right\}(T_0 - T)$$

$$\left.\left(\frac{\partial S_0}{\partial t}\right)\right|_{nudging} = \alpha_S\left\{\frac{\partial}{\partial x}\left(A\frac{\partial}{\partial x}\right)+\frac{\partial}{\partial y}\left(A\frac{\partial}{\partial y}\right)\right\}(S_0 - S)$$

$$\left.\left(\frac{\partial u}{\partial t}\right)\right|_{nudging} = \left\{\frac{\partial}{\partial x}\left(\mu\frac{\partial}{\partial x}\right)+\frac{\partial}{\partial y}\left(\mu\frac{\partial}{\partial y}\right)\right\}(u - U)$$

$$\left.\left(\frac{\partial v}{\partial t}\right)\right|_{nudging} = \left\{\frac{\partial}{\partial x}\left(\mu\frac{\partial}{\partial x}\right)+\frac{\partial}{\partial y}\left(\mu\frac{\partial}{\partial y}\right)\right\}(v - V)$$

Regional model receives from GCM:

- Initial conditions: T, S, u, v, U, V, η
- Liquid boundary conditions for T, S, η and normal component of barotropic velocity (U, V)
- T and S via second order relaxation terms

$$\left.\left(\frac{\partial T}{\partial t}\right)\right|_{nudging} = \left\{\frac{\partial}{\partial x}\left(A\frac{\partial}{\partial x}\right)+\frac{\partial}{\partial y}\left(A\frac{\partial}{\partial y}\right)\right\}(T - T_0)$$

$$\left.\left(\frac{\partial S}{\partial t}\right)\right|_{nudging} = \alpha_S\left\{\frac{\partial}{\partial x}\left(A\frac{\partial}{\partial x}\right)+\frac{\partial}{\partial y}\left(A\frac{\partial}{\partial y}\right)\right\}(S - S_0)$$

Серия окраинных морей Арктики

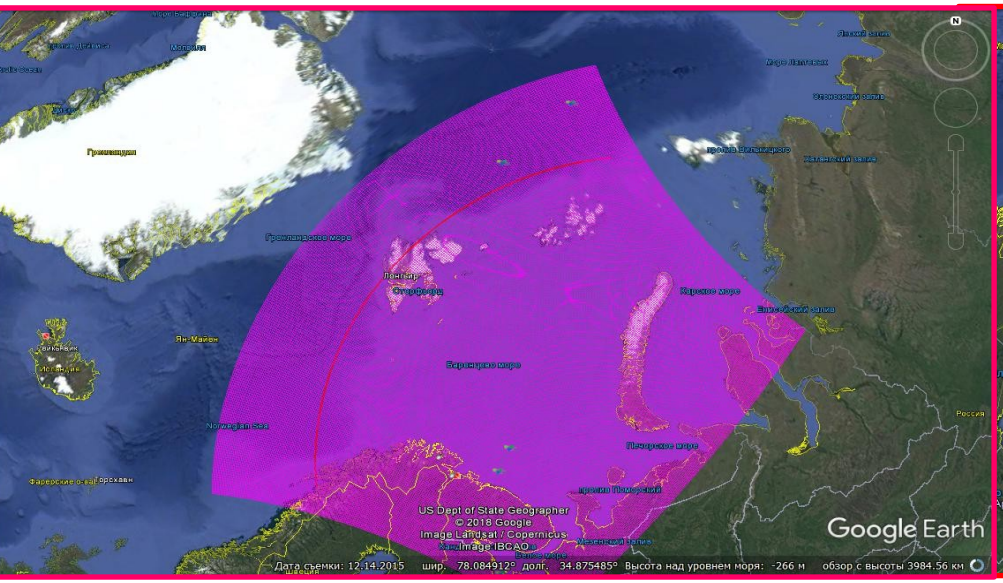

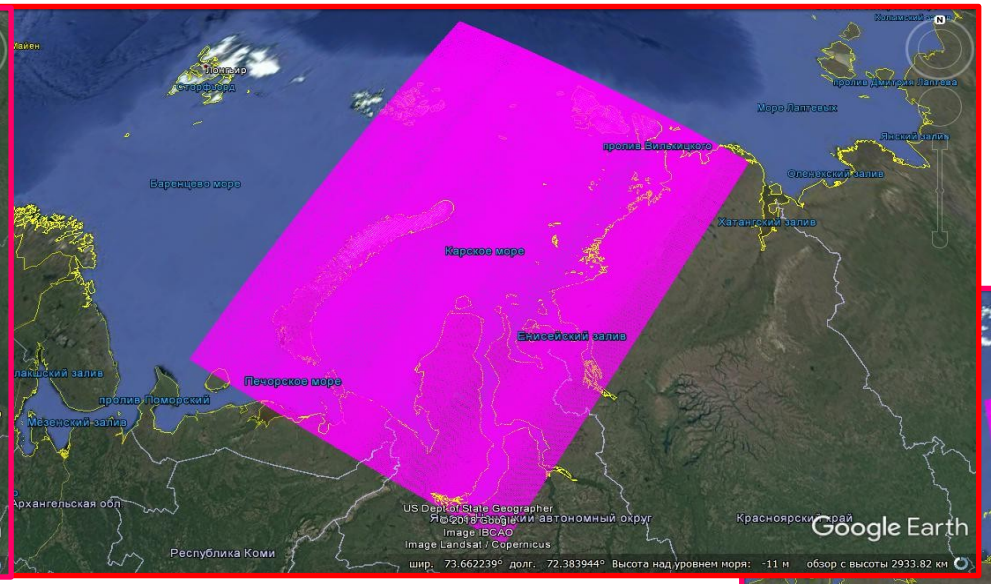

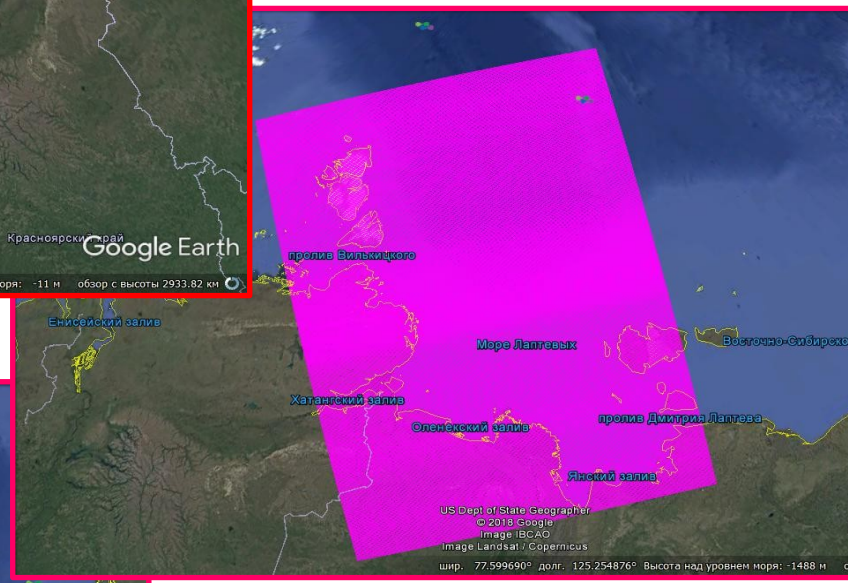

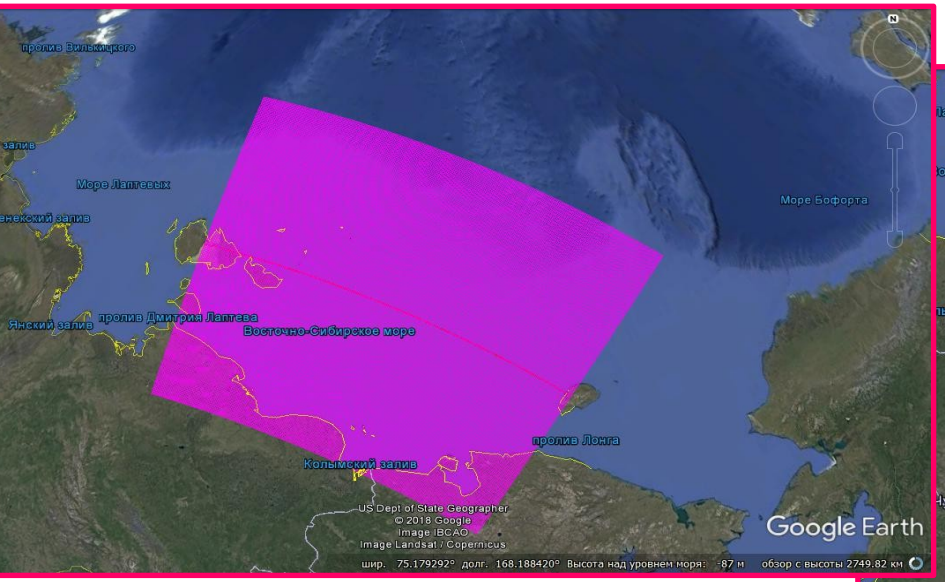

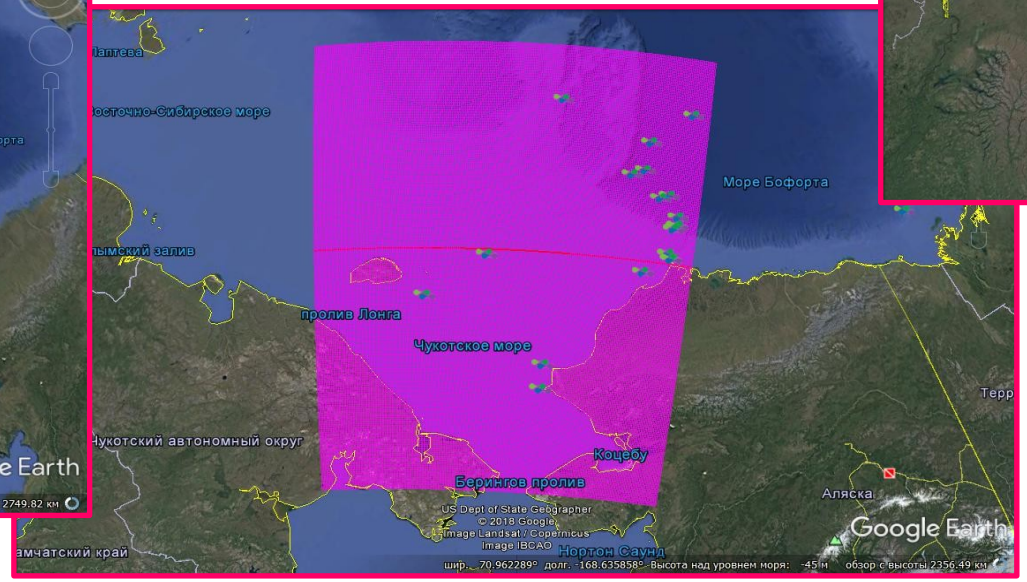

Процессор Cerebras WSE-2 — 850 тысяч ядер, 7 нм и энергопотребление 15 кВт

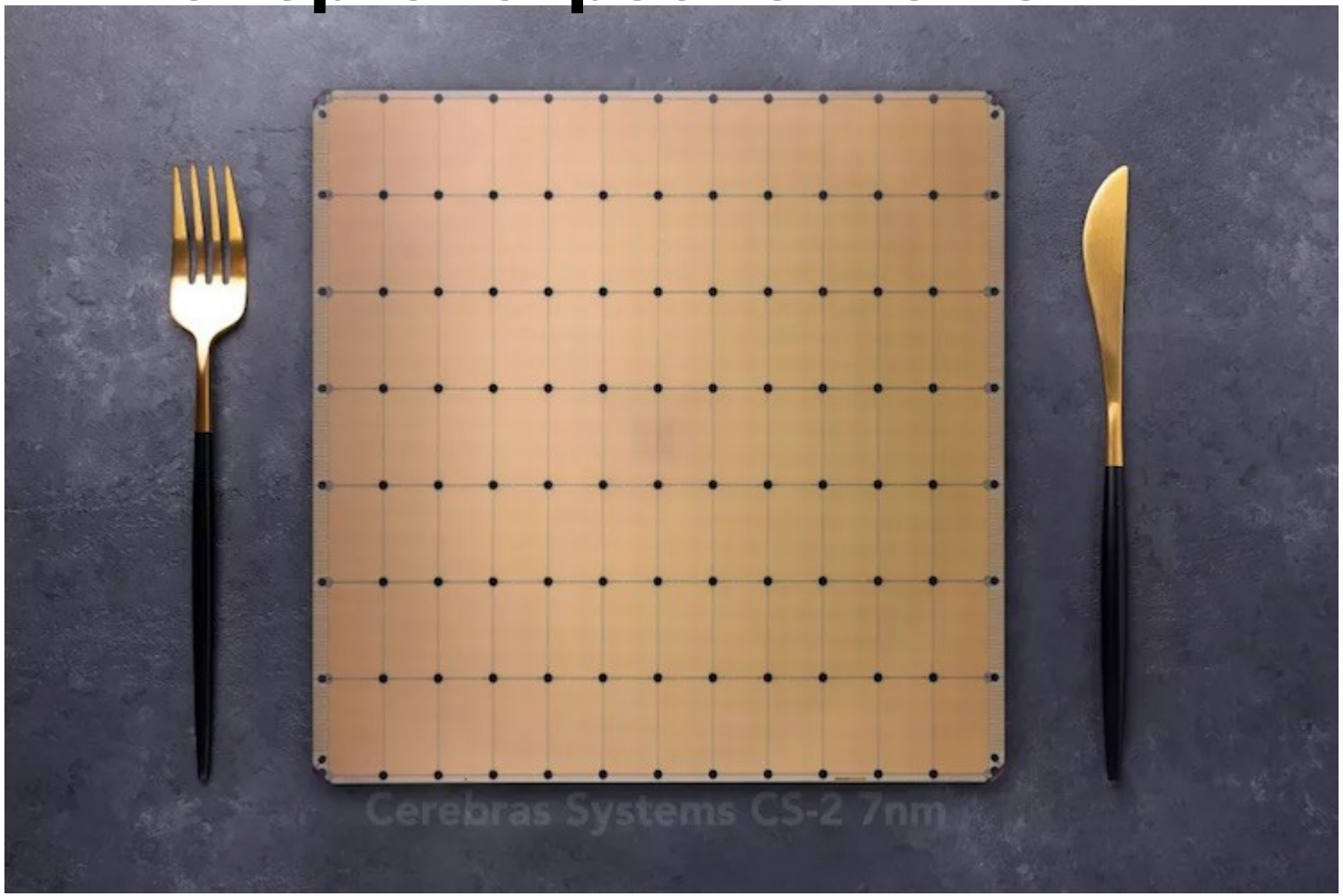

https://3dnews.ru/1037764/cerebras-predstavila-ogromniy-protsessor-wse2-850-tisyach-yader-7-nm-i-energopotreblenie-15-kvt

geosciences

MDPI

Article

Characteristics of Atmospheric Circulation Associated with Variability of Sea Ice in the Arctic

Gennady Platov *, Dina Iakshina and Vladimir Krupchatnikov

Institute of Computational Mathematics and Mathematical Geophysics, SB RAS, Novosibirsk 630090, Russia; iakshina.dina@sscc.ru (D.I.); krupchatnikov@sscc.ru (V.K.)

* Correspondence: plat@ommfao.sscc.ru

Received: 22 July 2020; Accepted: 4 September 2020; Published: 6 September 2020

check for updates

Abstract: The paper investigates the role of atmospheric circulation in the surface layer in forming the Arctic ice structure. For the analysis, the empirical orthogonal function (EOF) method of decomposition of the surface wind field is used, and the reaction of ice to changes in the principal components of leading EOF modes is investigated using statistical methods. Analyzing the rate of ice change in the Arctic associated with the Arctic ocean oscillation mode, we concluded that this mode's variability leads to the formation of a seesaw in the ice field between two regions. From the one side, it is the region of the central deep-water part of the Arctic, including the East Siberian Sea, and from the other side, it is all other marginal seas. The second ("dipole") mode is most associated with an increase/decrease in the ice thickness at the Arctic exit through the Fram Strait, as well as the formation of the so-called "ice factory" in the coastal region of the Beaufort Sea in the positive phase of this mode. There is also a significant relationship between the variability of third mode and the arrival of Atlantic waters with a high heat content into the Arctic through the Barents opening, which creates preconditions for ice formation in this region.

Поле ветра в район СЛО в период с 194 по 2019

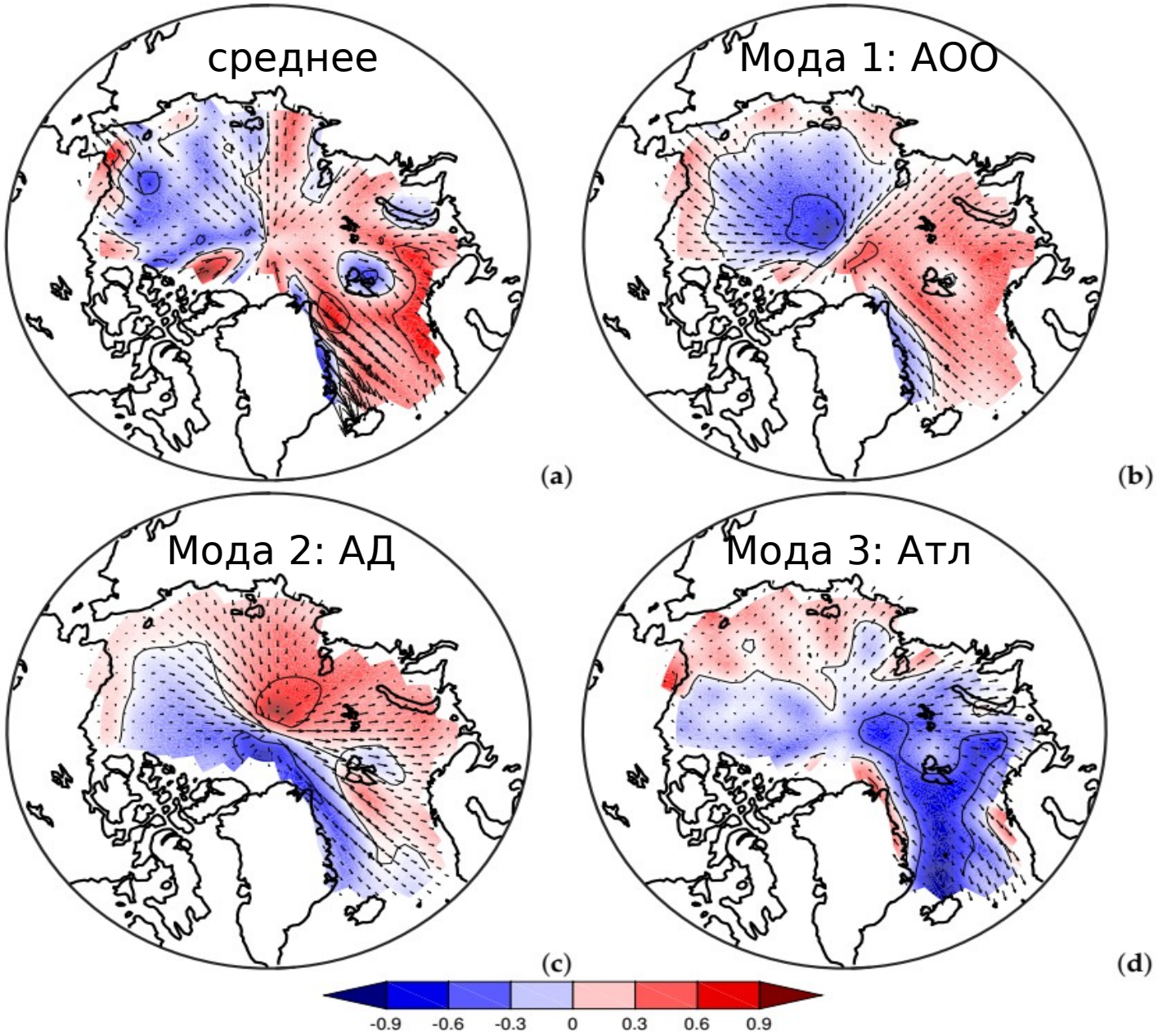

Figure 2. The average value and three eigenfunctions of the surface wind EOF decomposition (arrows) and its vorticity (color and contours): (**a**) averaged from 1948 to 2019 spatial distribution of the wind field, (**b**) the first eigenfunction of the surface wind speed, (**c**) the second, (**d**) the third.

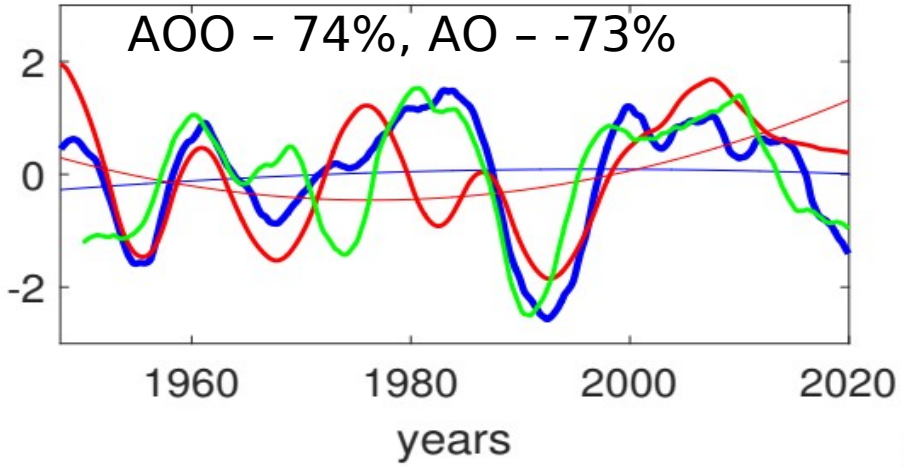
AOO – 74%, AO – -73%
2
0
-2
1960
1980
2000
2020
years

(a)

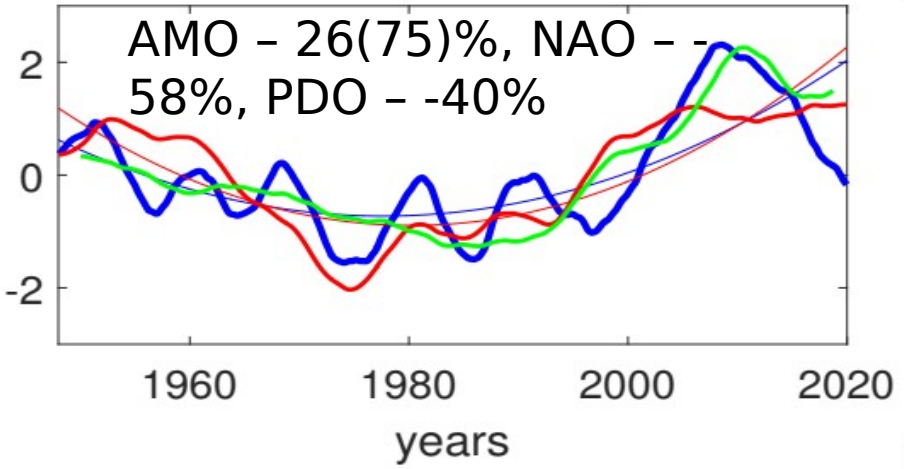
AMO – 26(75)%, NAO – -
58%, PDO – -40%
2
0
-2
1960
1980
2000
2020
years

(b)

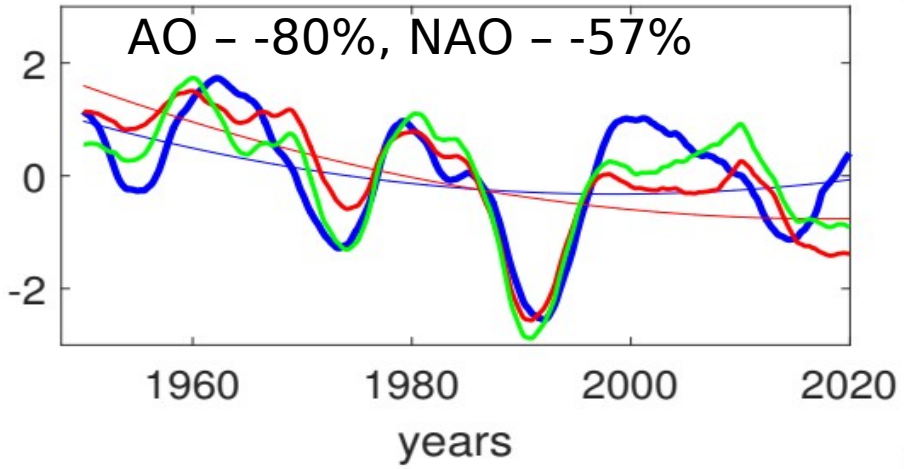
AO – -80%, NAO – -57%
2
0
-2
1960
1980
2000
2020
years

(c)

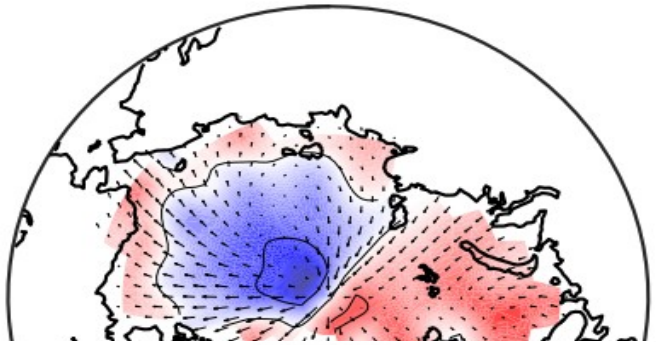

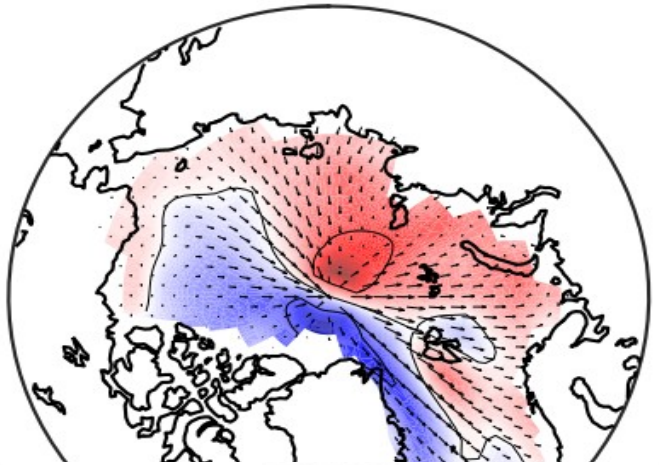

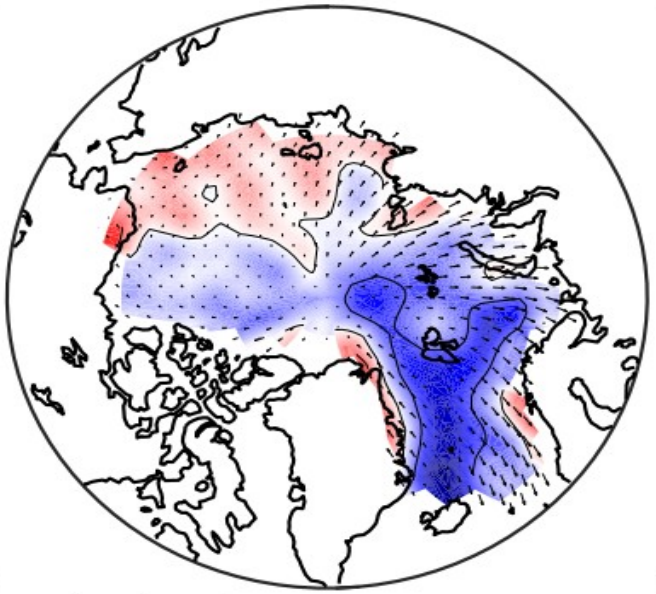

(c

Изменения скорости роста льда при переходе от отрицательной фазы моды к положительной

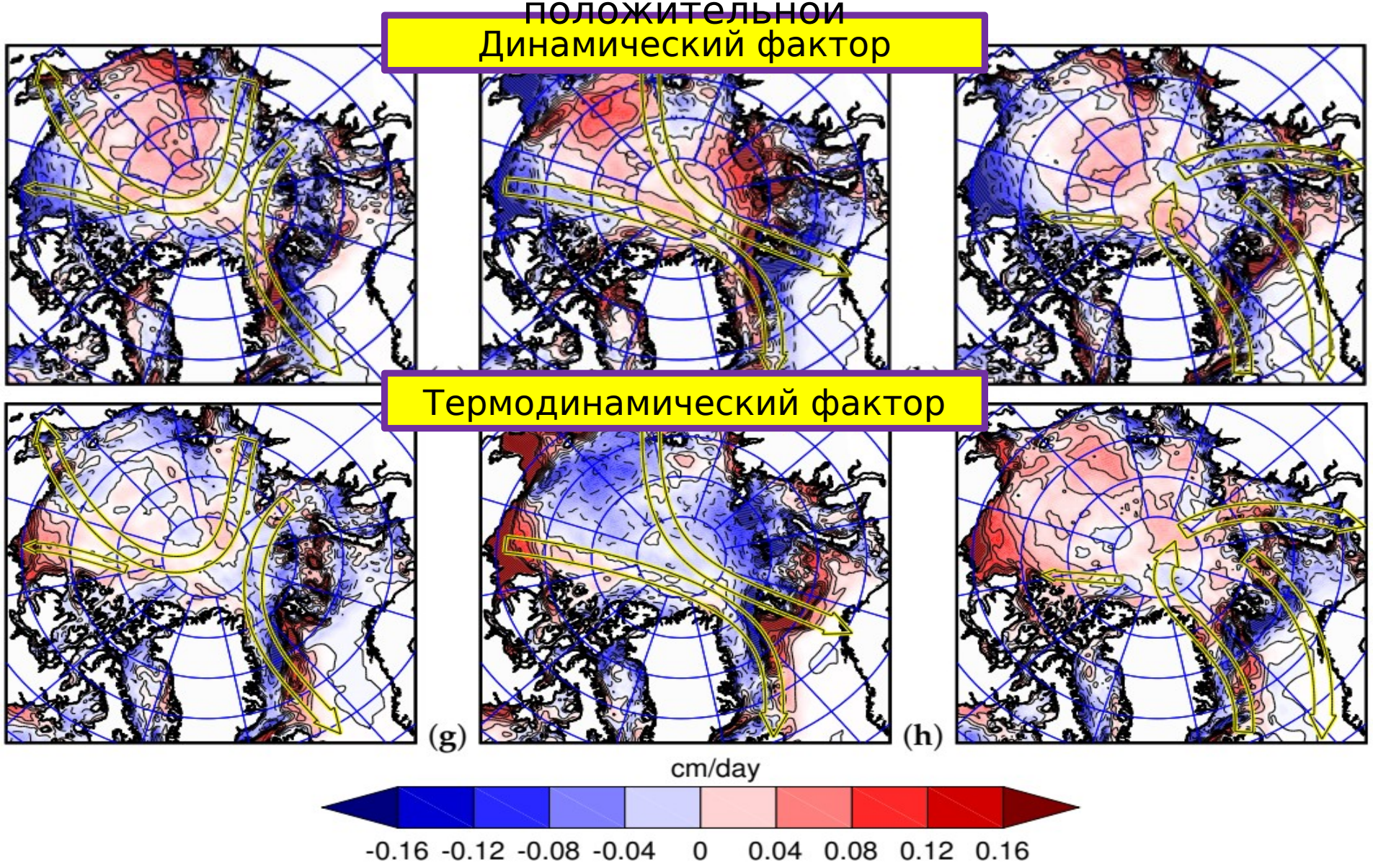

Characteristics of mesoscale eddies of Arctic marginal seas: results of numerical modeling

Gennady Platov and Elena Golubeva

Institute of Computational Mathematics and Mathematical Geophysics SB RAS, 630090, Lavrentiev prospekt 6, Novosibirsk, Russia

E-mail: platov.g@gmail.com, e.golubeva.nsk@gmail.com

Abstract. A simple method is proposed for identifying mesoscale eddies in the results of numerical modeling. The method uses extrema in distributions of the sea level elevation as eddy markers. By using the method, we analyze statistics of mesoscale eddies resulting from SibPOM numerical simulations in the Eurasian sector of the Arctic marginal seas. The results of using this method show that the number of cyclonic eddies slightly exceeds the number of anticyclonic eddies, but the excess is only 2-3%. Also, we demonstrate that a significant number of eddies arise under the ice cover. The number of such eddies increases significantly in winter. This fact indicates that the convection caused by salt rejection during freezing plays an essential role in their formation. The numerical modeling results confirm the phenomenon of active eddy generation in the ice edge zone. Besides, the results show that in the near-edge zone, a more significant number of eddies are formed from the icy side adjacent to the edge, and not from the ice-free side. The periods of seawater freezing and ice melting, accompanied by corresponding displacements in the ice edge, produce eddies different in nature. The number of eddies in the marginal ice zone has two seasonal maxima corresponding to these two periods.

Eddy identification with length-scale d

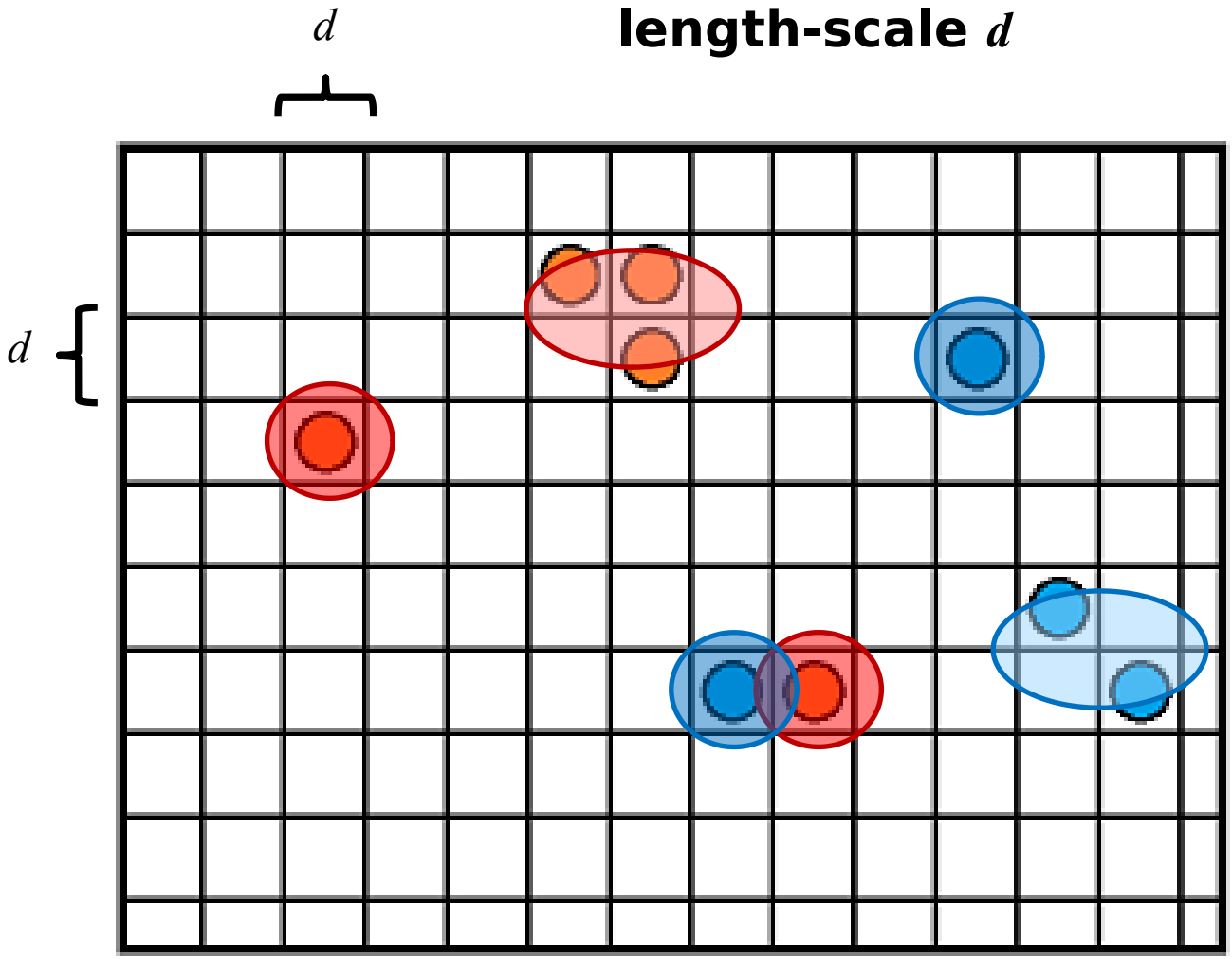

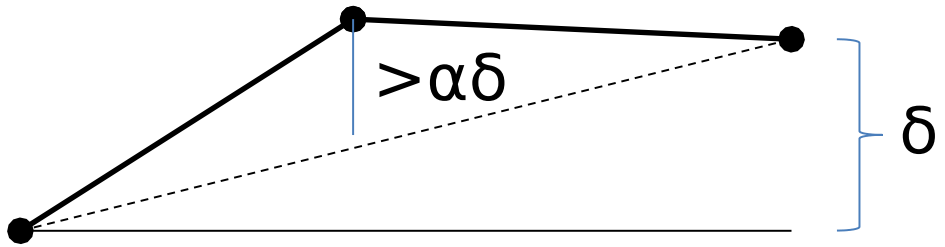

$$\begin{cases} \eta_{i,j} - \dfrac{\eta_{i-1,j} + \eta_{i+1,j}}{2} > \alpha \left| \eta_{i-1,j} - \eta_{i+1,j} \right| \\ \eta_{i,j} - \dfrac{\eta_{i,j-1} + \eta_{i,j+1}}{2} > \alpha \left| \eta_{i,j-1} - \eta_{i,j+1} \right| \end{cases}$$

Averaged number of mesoscale eddies (x10³)

	1	2	3	4	5	6	7	8	9	10	11	12
Barents Sea	3.8	3.8	3.9	3.8	3.8	3.5	3.3	3.1	3.1	3.4	3.6	3.8
	3.6	3.5	3.6	3.5	3.5	3.1	2.9	2.7	2.7	3.0	3.2	3.5
Kara Sea	1.9	2.1	2.1	2.2	2.1	1.9	1.7	1.6	1.5	1.5	1.7	1.8
	1.8	1.9	1.9	1.9	1.9	1.7	1.4	1.4	1.3	1.4	1.5	1.7
Laptev Sea	1.5	1.5	1.5	1.4	1.3	1.3	1.1	1.1	1.1	1.3	1.5	1.5
	1.4	1.3	1.3	1.2	1.1	1.0	0.9	0.9	0.9	1.1	1.3	1.3
East Siberian Sea	1.5	1.6	1.8	1.8	1.8	1.7	1.3	1.1	1.0	1.1	1.3	1.4
	1.4	1.5	1.7	1.6	1.7	1.6	1.2	0.9	0.8	1.0	1.2	1.3
Chukchi Sea	2.4	2.3	2.3	2.1	1.8	1.7	1.8	1.9	2.1	2.2	2.2	2.2
	2.3	2.2	2.2	2.1	1.7	1.7	1.6	1.8	2.0	2.1	2.1	2.1
Total	11.											
	10.											

Cyclonic

Anticyclonic

	1	2	3	4	5	6	7	8	9	10	11	12
Barents Sea	2.6	2.3	2.4	2.1	2.2	2.0	2.3	2.4	2.6	2.7	2.7	2.6
2.42/2.19	2.4	2.1	2.2	2.0	2.0	1.8	2.0	2.1	2.3	2.4	2.4	2.4
Chukchi Sea	0.0	0.0	0.0	0.0	0.0	0.03	0.4	1.0	1.2	1.3	0.6	0.03
0.38/0.36	0.0	0.0	0.0	0.0	0.0	0.03	0.4	0.9	1.2	1.2	0.6	0.03

Eddies in the ice edge zone

Chukchi Sea

	6	7	8	9	10	11	12
Ice cover is 10-50%	10	131	207	244	82	128	60
72/69	8	125	191	233	83	121	57
Ice cover is 50-80%	37	223	407	374	48	142	121
114/109	30	205	384	364	48	141	122

Cyclonic

Anticyclonic

$$\approx 1.5$$

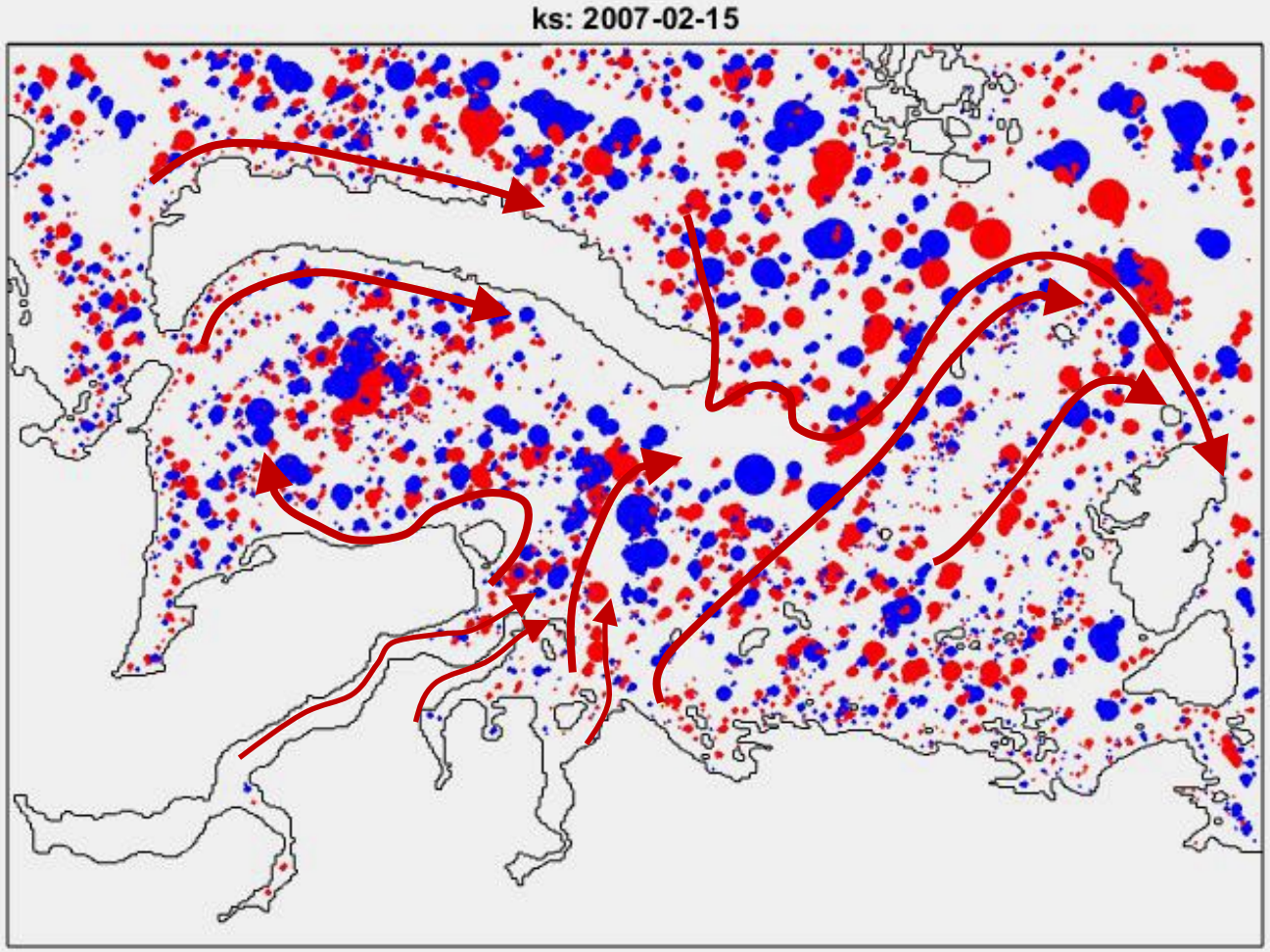

Eddies identified in Kara Sea region

Cascading and eddies: St. Anna Through

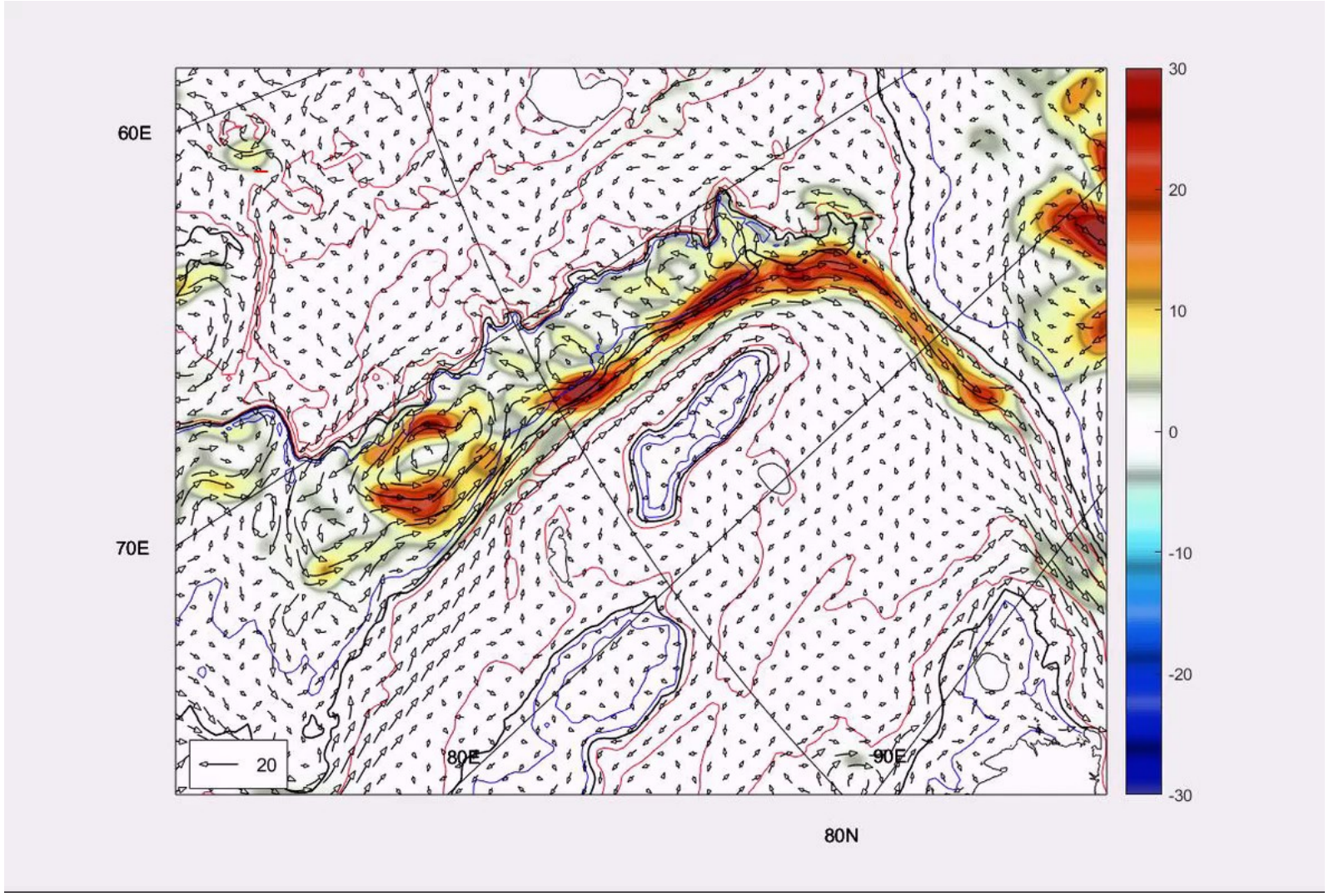

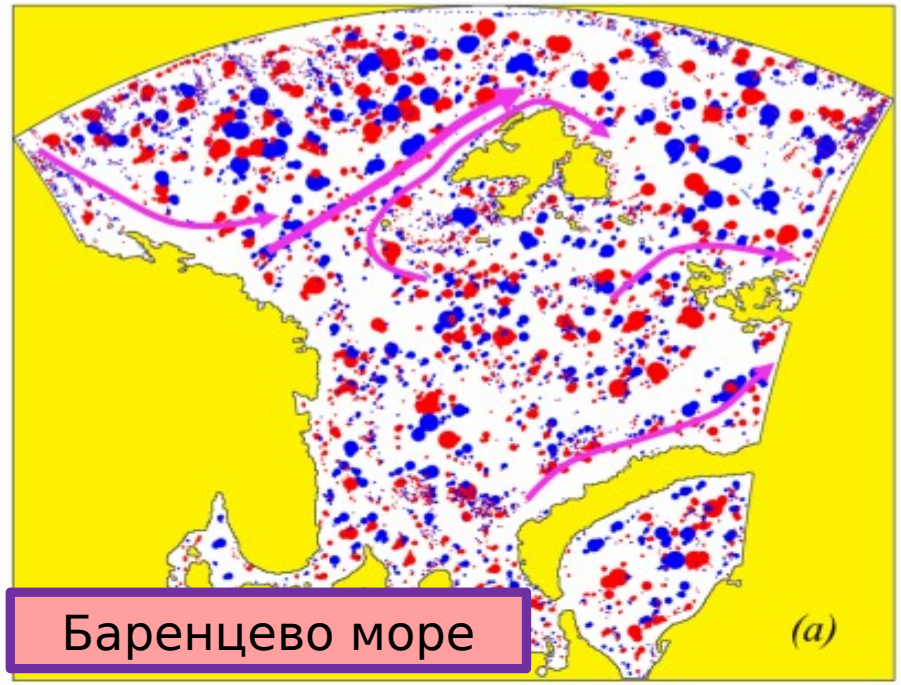

Баренцево море

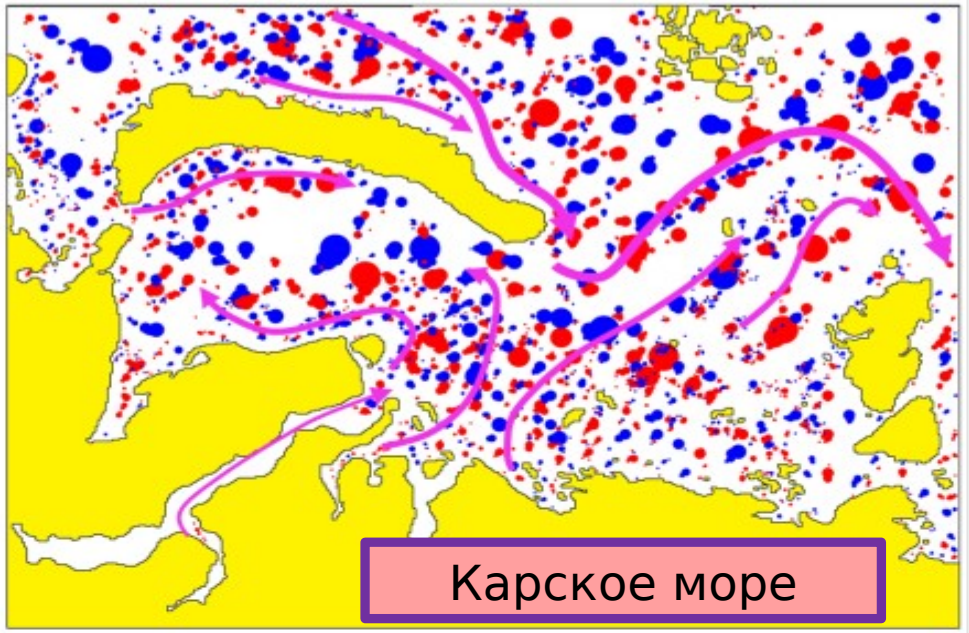

Карское море

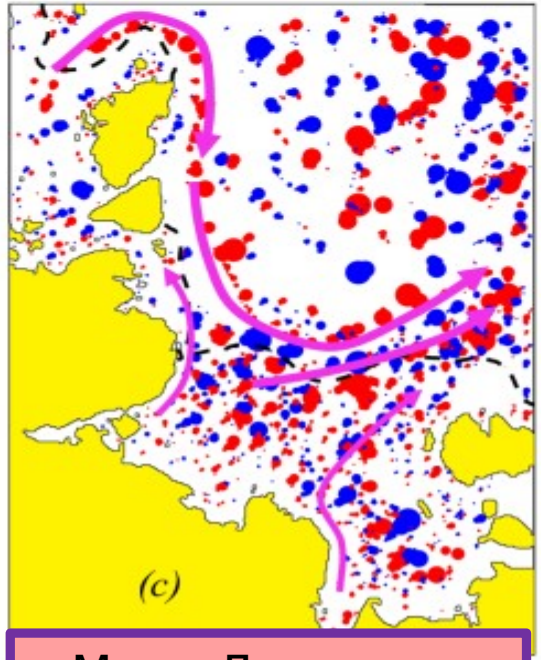

Море Лаптевых

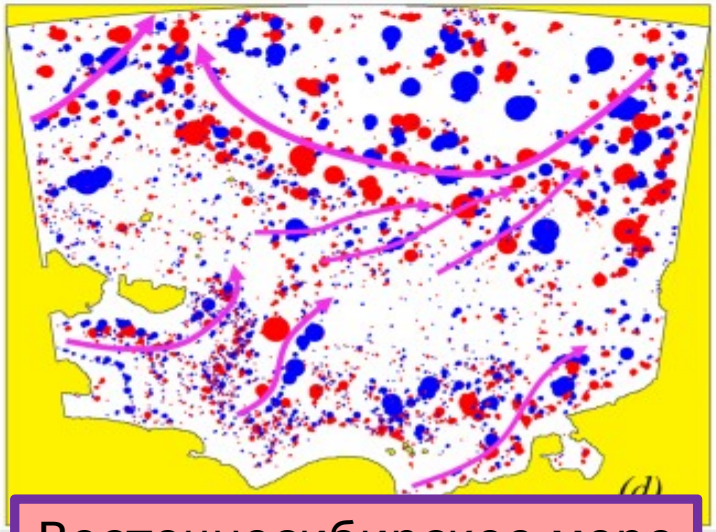

Восточносибирское море

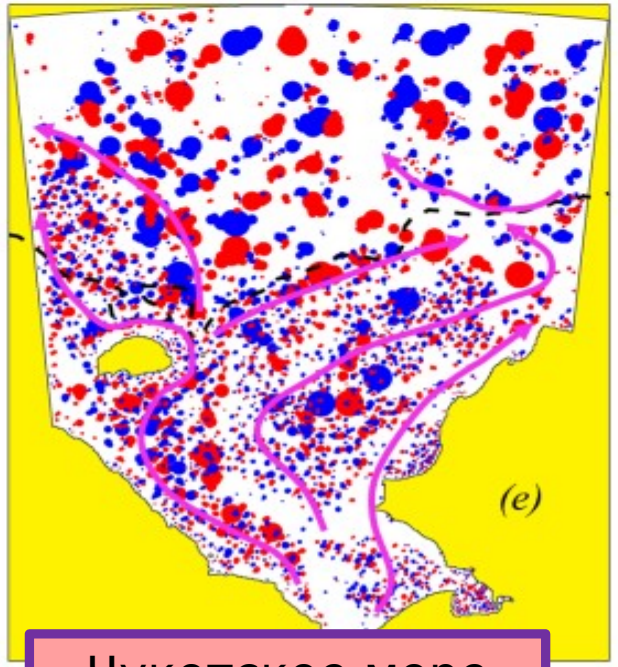

Чукотское море

Main modes of the Arctic Ocean circulation and a relationship between their trends and the Atlantic water heat content

Gennady Platov, Marina Kraineva and Elena Golubeva

Institute of Computational Mathematics and Mathematical Geophysics SB RAS, 630090, Lavrentiev prospekt 6, Novosibirsk, Russia

E-mail: platov.g@gmail.com, krayneva-m@yandex.ru, e.golubeva.nsk@gmail.com

Abstract. A study is presented on integral variability in Arctic Ocean characteristics, such as the volume transport and the heat content of the Atlantic water (AW) layer, obtained as results of numerical simulations using a model, SibCIOM. On the basis of an EOF decomposition three non-degenerate modes are obtained for the integral stream function and three modes for the heat content of the AW layer in the Arctic. Considering the cross-correlations of the EOF principal components a 44-yr cycle is obtained. It relates the cyclonic circulation mode in the Arctic and the second mode of AW heat content, associated with the AW warming in the area of the Beaufort Gyre. The Atlantic Multi-decadal Oscillation (AMO) statistically can act as a source of such a cycle, however, the thus obtained correlation is at the limit of the admissible significance, and the period of AMO oscillations is 1.5-2 times longer. In our opinion, a relationship with fluctuations in the Atlatic Meridional Overturning Circulation (AMOC) seems to be more plausible. However, no understanding of the role of these two mid-latitude and polar processes in relation to what extent they act as a cause or a consequence has yet been established in this study.

EOF decomposition of stream function

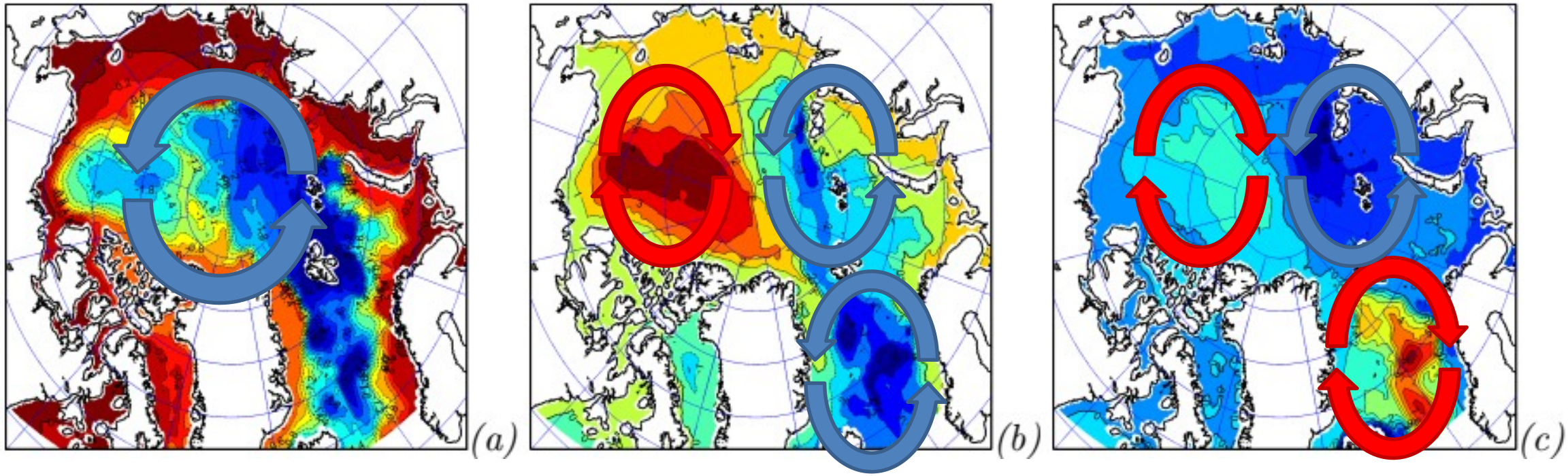

SF1 SF2 SF3

Arctic Ocean circulation

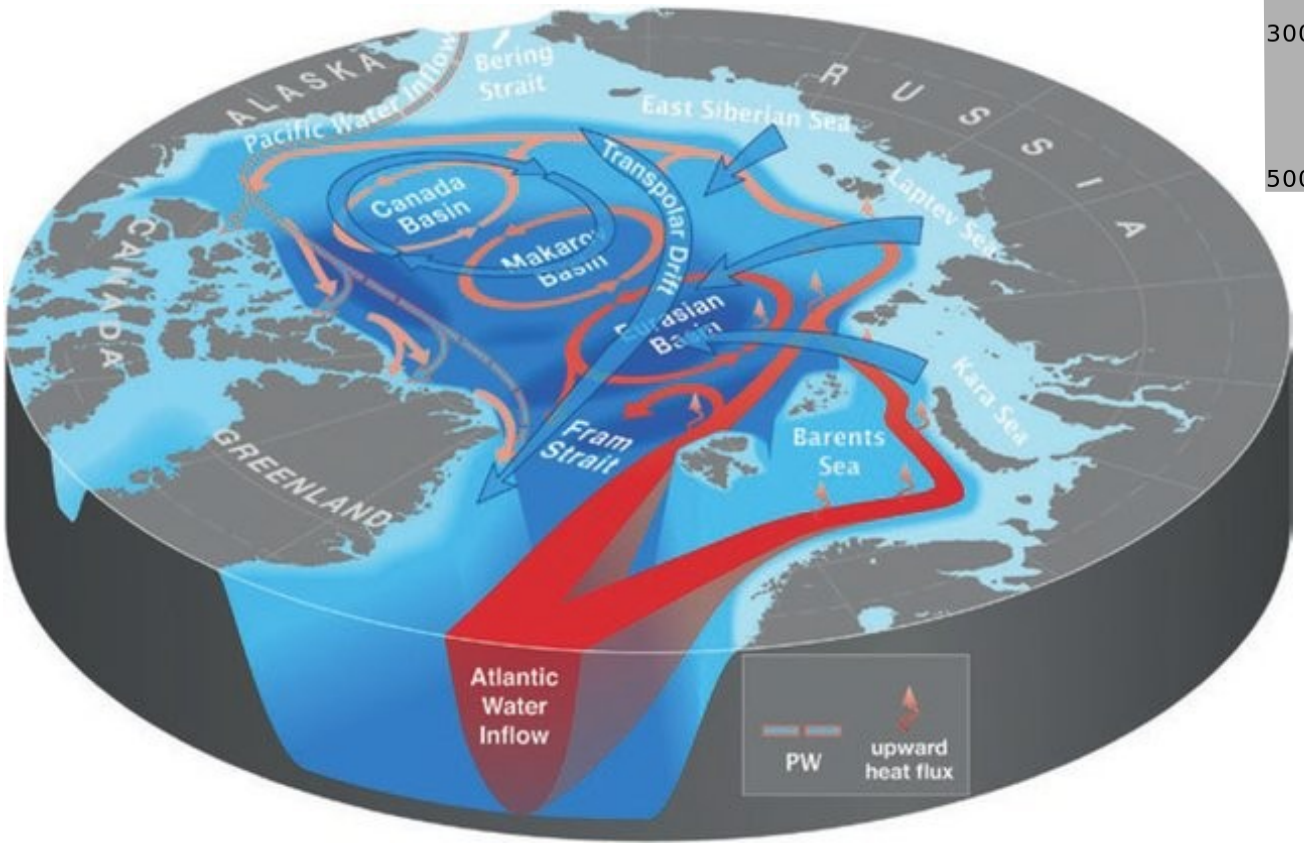

(reproduced from Carmack et al. 2015)

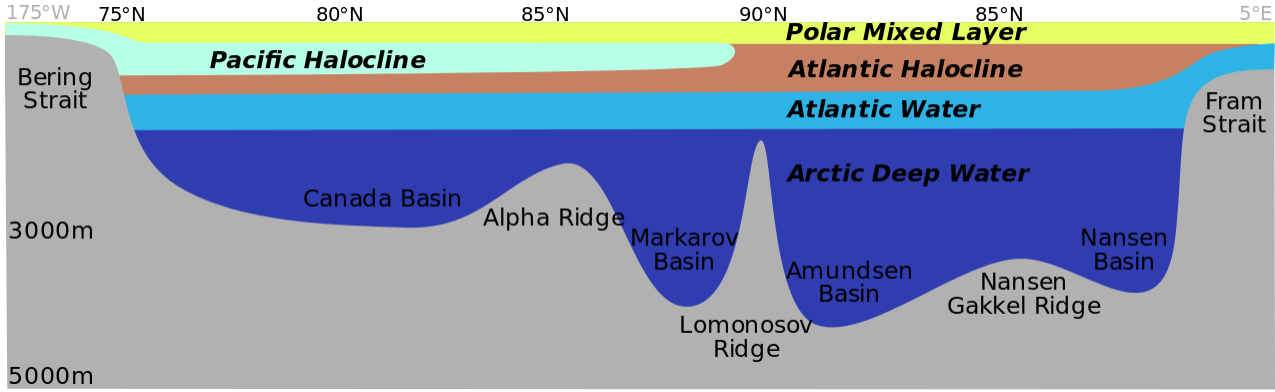

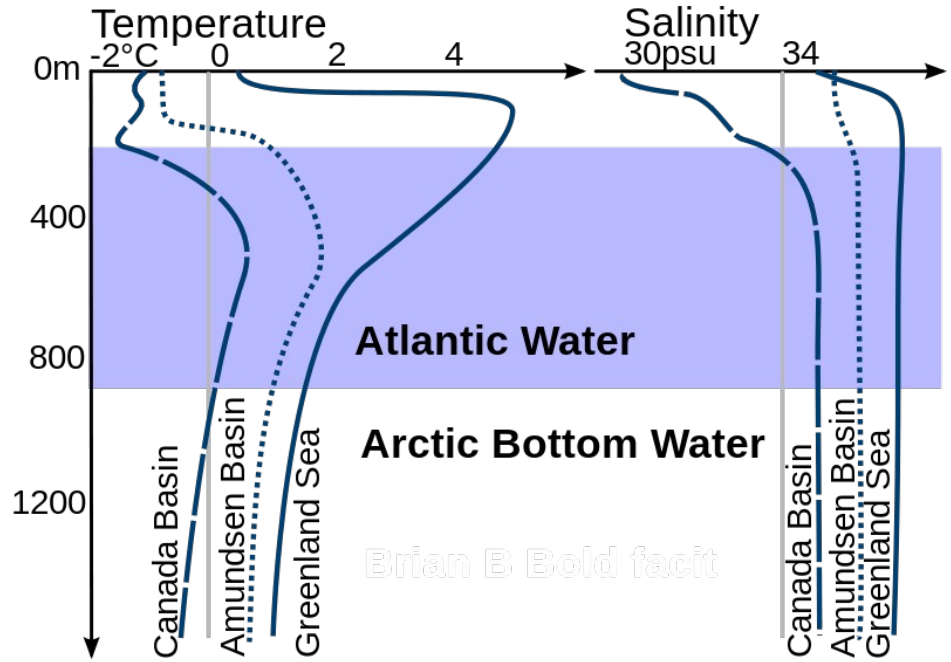

https://commons.wikimedia.org/w/index.php?curid=21129204

AW heat content

$$HC(x,y,t) = \int_{h_l}^{h_u} c_p \rho T(x,y,z,t) dz$$

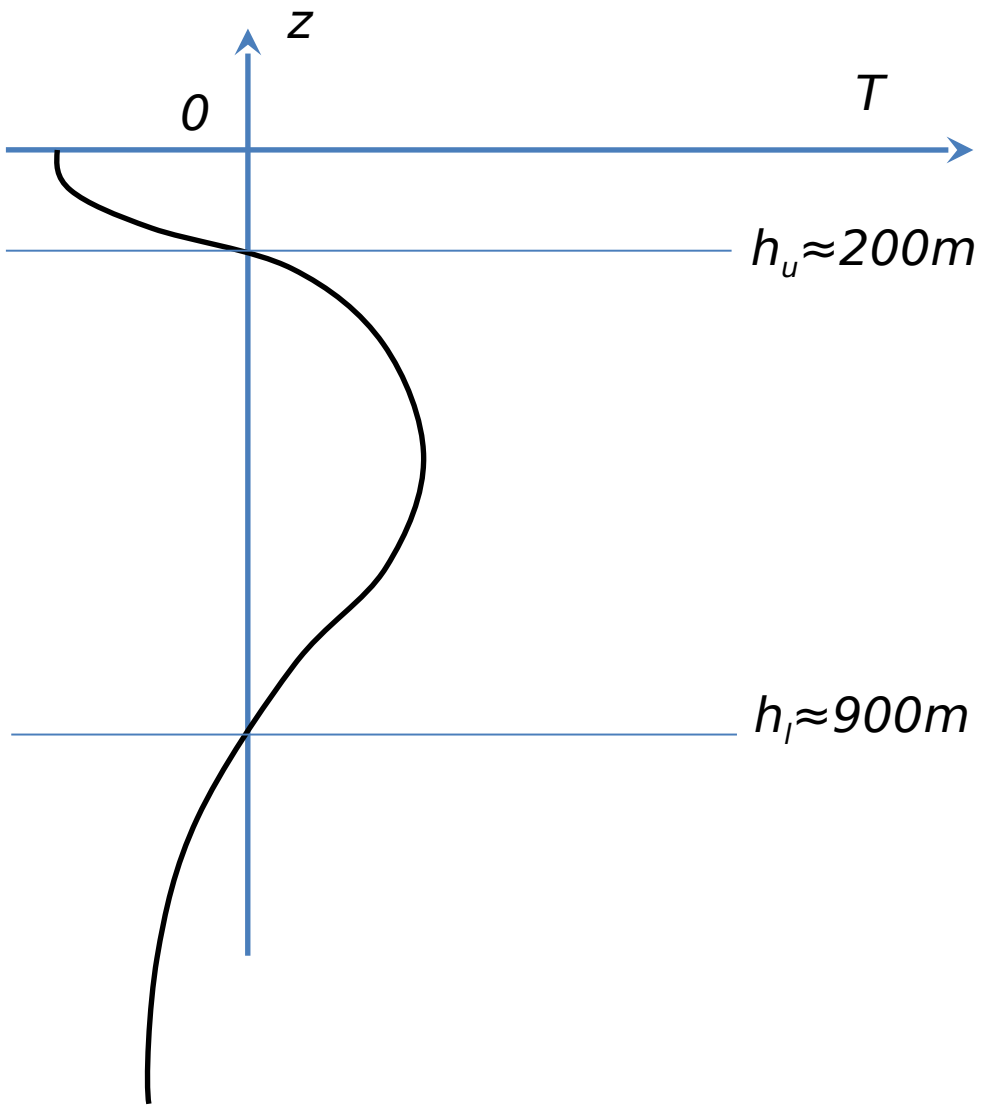

EOF decomposition of AW heat content

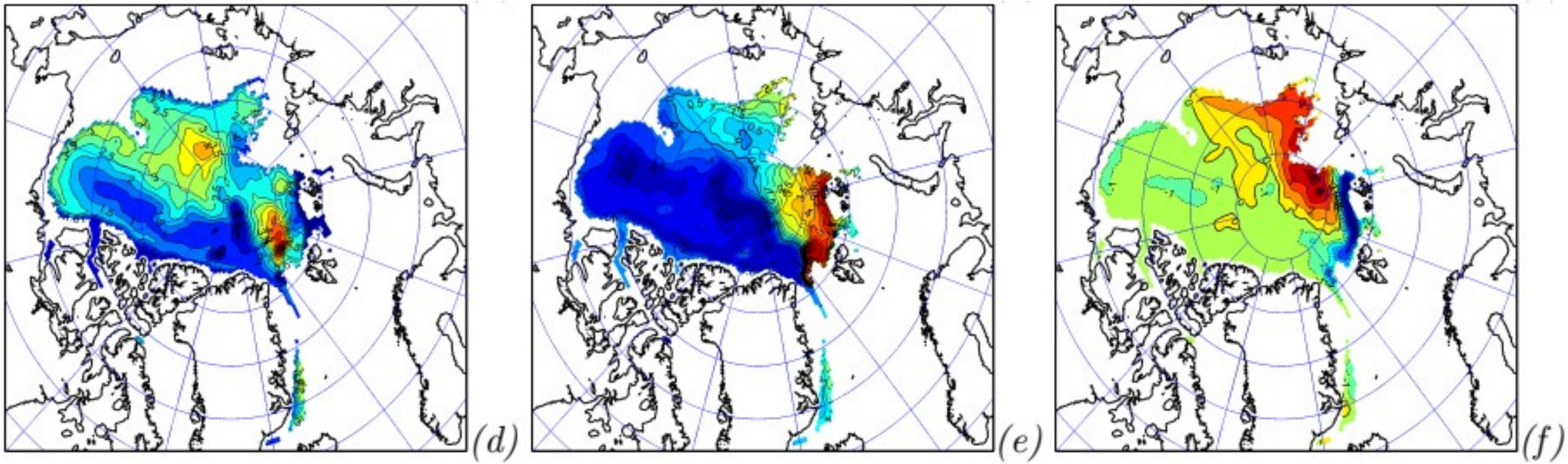

Q1 Q2 Q3

Correlations SF and Q modes

	SF1	SF2	SF3
Q1	21 60/6	15	-34 -54/-13
Q2	10 -78/13 73/-9	-52 -85/2	2 48/2
Q3	4 20/4	-12 -67/14	2 37/15

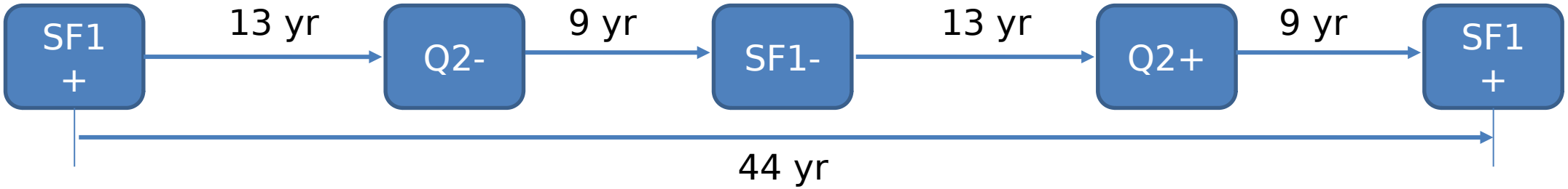

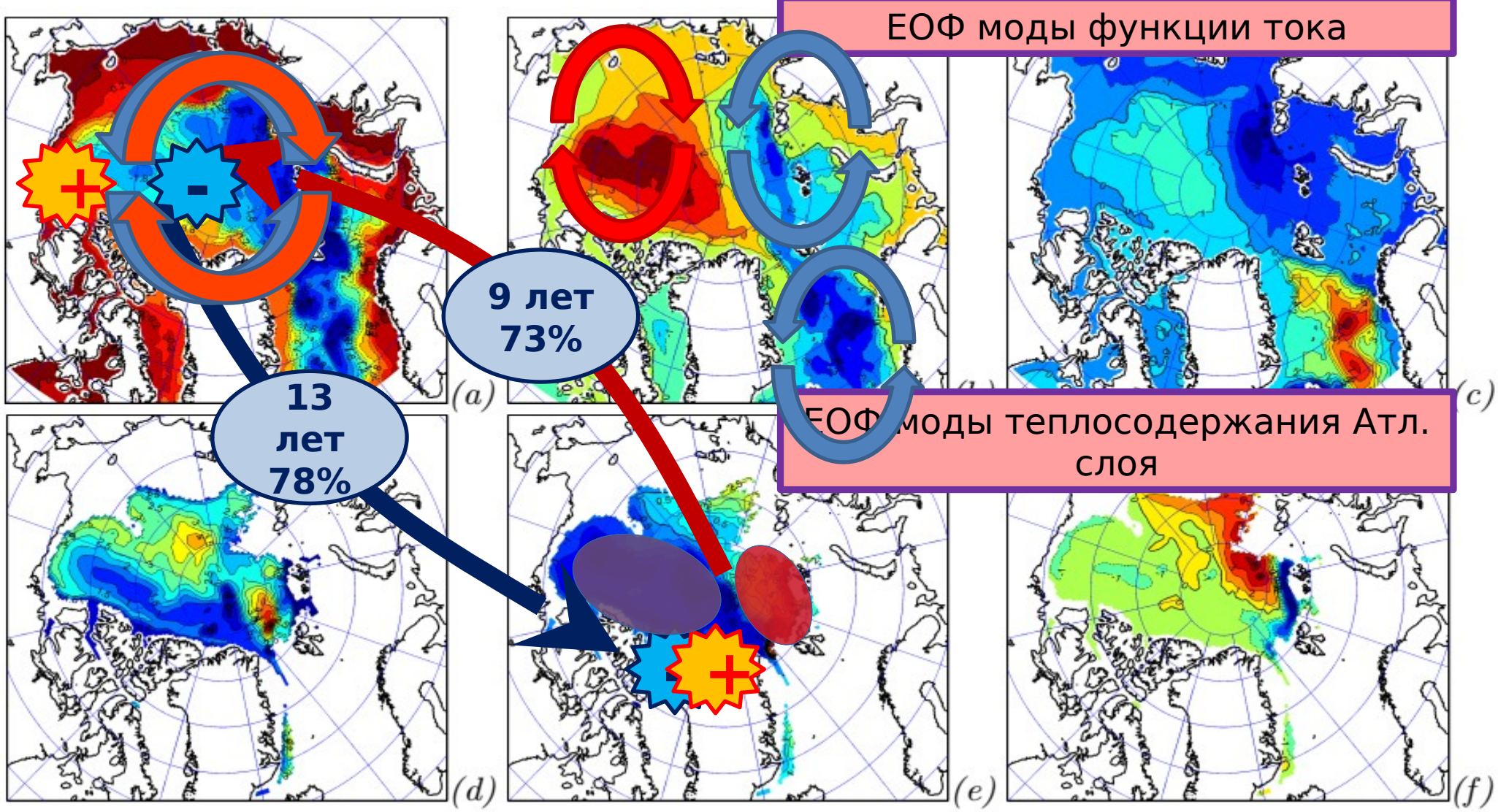

- A more significant reaction to a change in SF1 occurs after 13 years. We can trace it in the amplification of the opposite phase of Q2. The correlation coefficient is -78%. On the contrary, a change in Q2 leads with a correlation of 73% to a co-directional change in SF1 after 9 years. Thus, within these two modes (SF1 and Q2), we can trace a 44-yr cycle: positive SF1 - negative Q2 after 13 years - negative SF1 after 9 years - positive Q2 after 13 years - again positive SF1 after 9 years ...

Possible 44-yr oscillation origins

- AMO – Atlantic Multi-decadal Oscillation
  - 60-80 yr (corr -35%, time lag -19yr)
- AMOC – Atlantic Meridional Overturning Circulation
  - GFDL – 50 yr (Delworth et al., 1993, J. Climate)
  - ECHAM3-LSG – 35 yr (Timmermann et al., 1998, J. Climate)

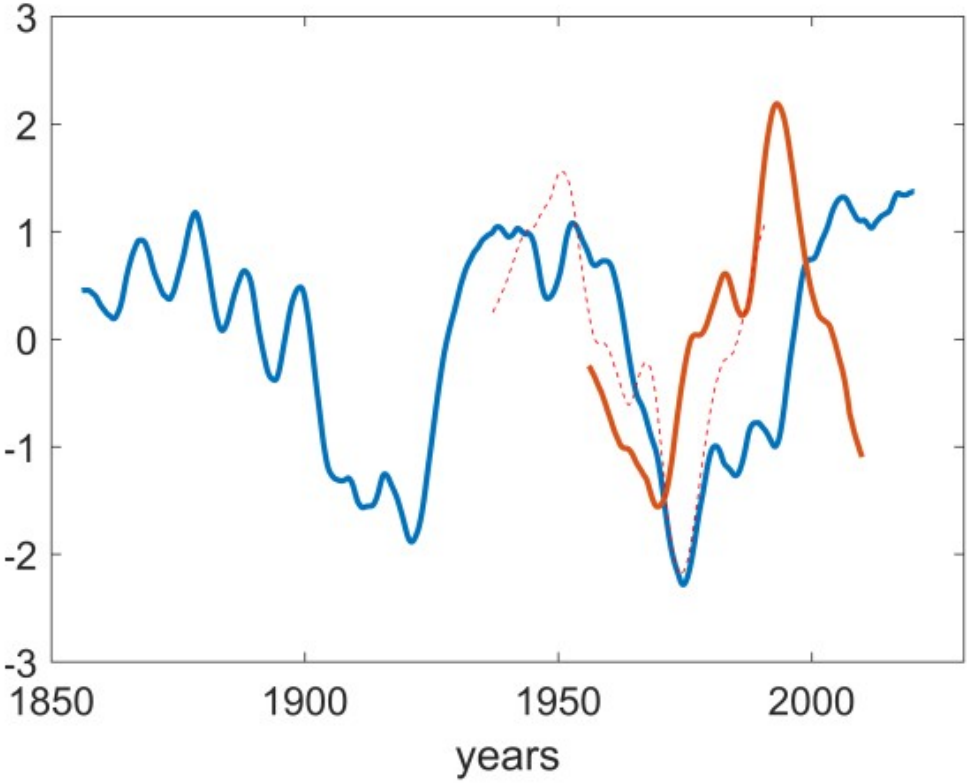

AMOC

$$W = \int_{-H}^{0} \int_{X_w}^{X_e} V^+ dx dz,$$

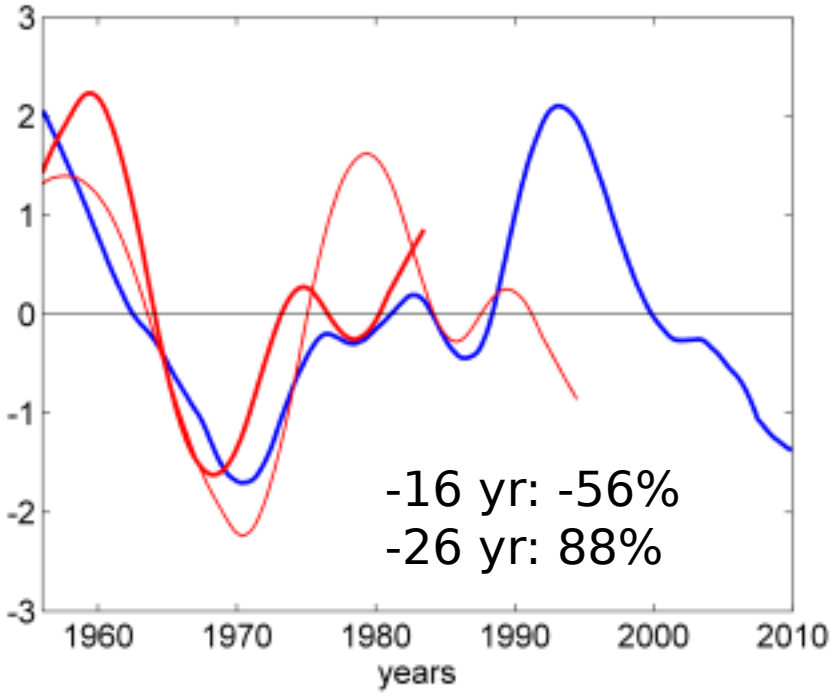

(c)

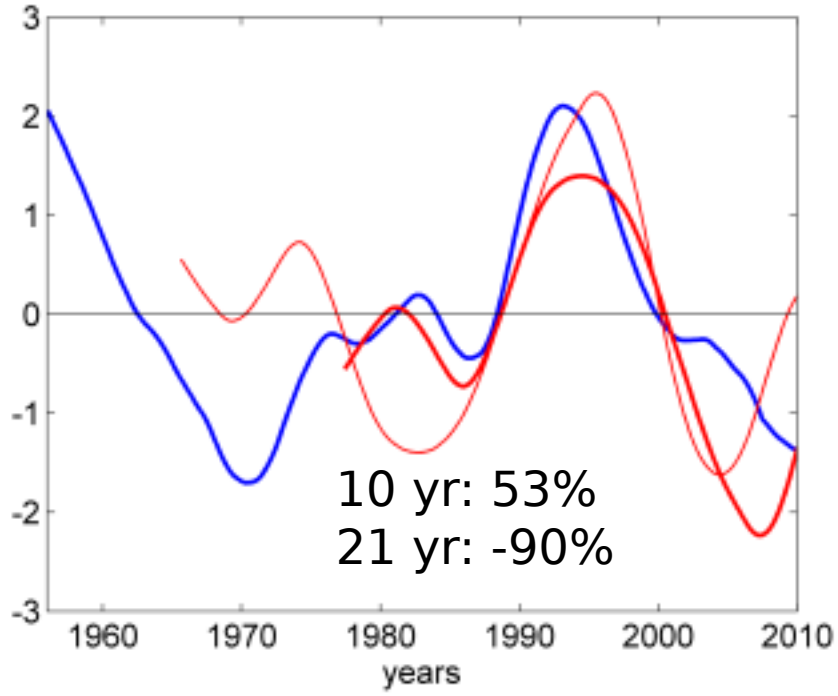

(d)

Спасибо!